Cerenkov Detectors

These are detectors designed to detect the light coherently emitted by the atoms along the path of a relativistic particle traversing a medium at velocity

$$v = \beta c$$

when v exceeds the speed of light in the medium, c/n , where n is the index of refraction of the medium.

The angle at which the light is emitted can be calculated using the relation between the distance traveled by the particle and by the emitted radiation in time t.

$$cos\ \Theta_c = \frac{(c/n)t}{\beta ct} = \frac{1}{\beta n}.$$

Θ_c is called the *Cerenkov* angle.

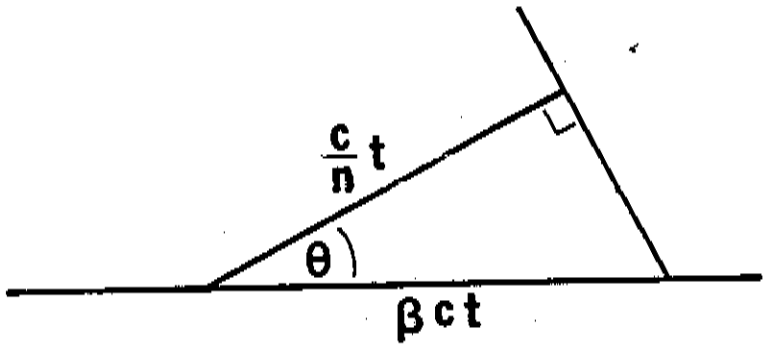

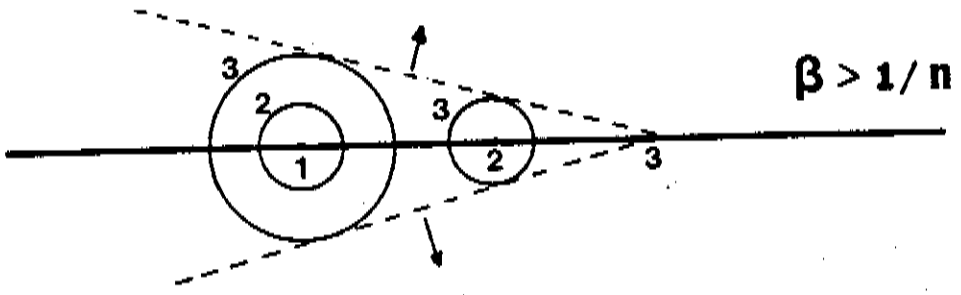

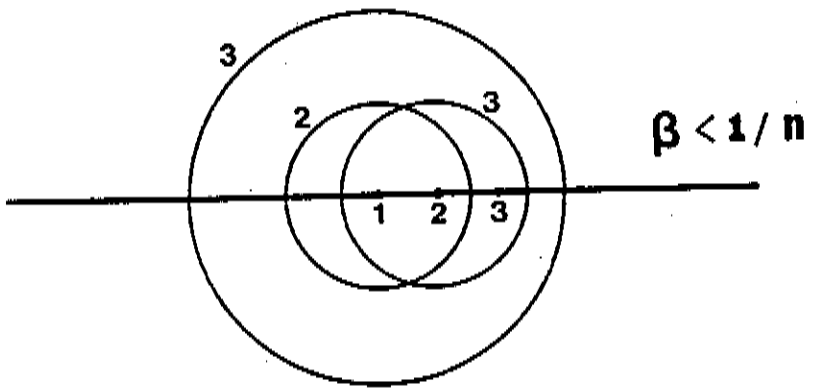

$$cos\ \Theta_c = \frac{1}{\beta n} < 1.0 \qquad \Rightarrow \qquad \beta > \frac{1}{n}$$

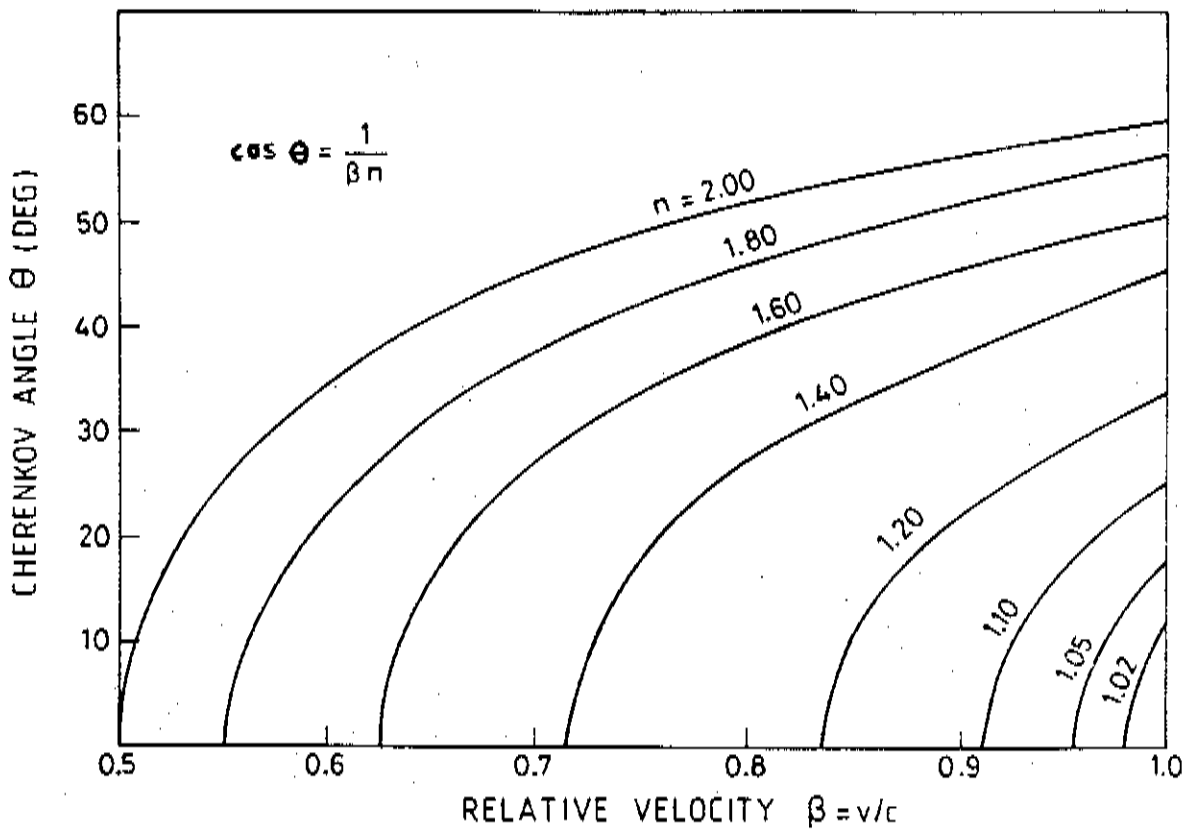

TYPICAL β's

Species	1 GeV/c	2 GeV/c
π	0.9904	0.9976
K	0.8967	0.9709
p	0.7293	0.9053

Maximum Cerenkov angle occurs for $\beta = 1$,

$$cos\ \Theta_c(max) = \frac{1}{n}.$$

Threshold Cerenkov Counter

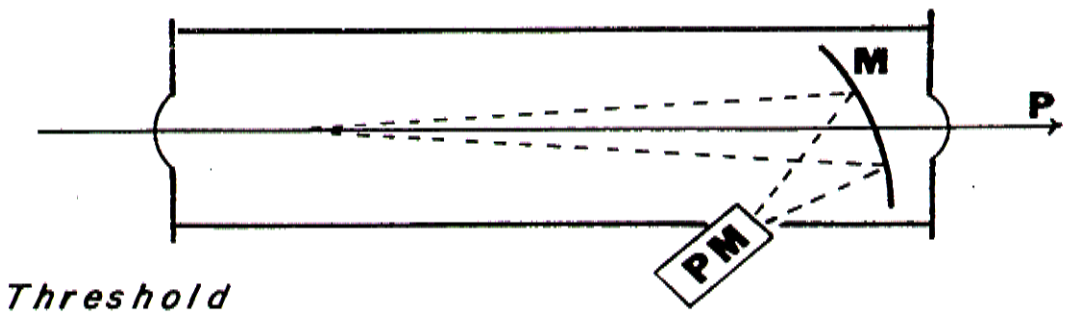

For a counter filled with material of index of refraction n, the *threshold* momentum, p_t, for a particle with mass, m, is given by

$$p_t = m\gamma_t\beta_t c = \frac{mc}{\sqrt{n^2-1}}.$$

Thus, p_t scales directly as the mass.

$$p_t(\pi) = 6GeV/c \;\Rightarrow\; p_t(K) \simeq 21GeV/c$$
$$\Rightarrow\; p_t(p) \simeq 40GeV/c$$

The number of photons emitted along the particle path, for $\lambda =$ 350-500 nm, the approximate range over which PMT's have good efficiency,

$$\frac{dN}{dx} = 390 \;\; sin^2\,\Theta_c \;\; photons/cm.$$

The index of refraction of a gas depends on the pressure, P,

$$n - 1 = (n_o - 1)\ \frac{P}{P_o},$$

where n_o and P_o refer to atmospheric pressure.

The index of refraction can be tuned to make the counter very efficient for the particle with mass, m, and momentum, p_t.

Since p.e. emission is Poisson-distributed,

$$\begin{aligned} \epsilon &= 1 - Pr(0, N_e) \\ &= 1 - e^{-N_e}, \end{aligned}$$

where $N_e \simeq 100\ sin^2\Theta_c$ photons/cm times the counter length (taking the collection efficiency and q.e. of the PMT into account). Since $Pr(0,5) = 0.01$, we need an average of 5 p.e. in the PMT for an efficiency of 99%. $sin^2\Theta_c$ is very small for β's we are interested in, so these counters tend to be quite long.

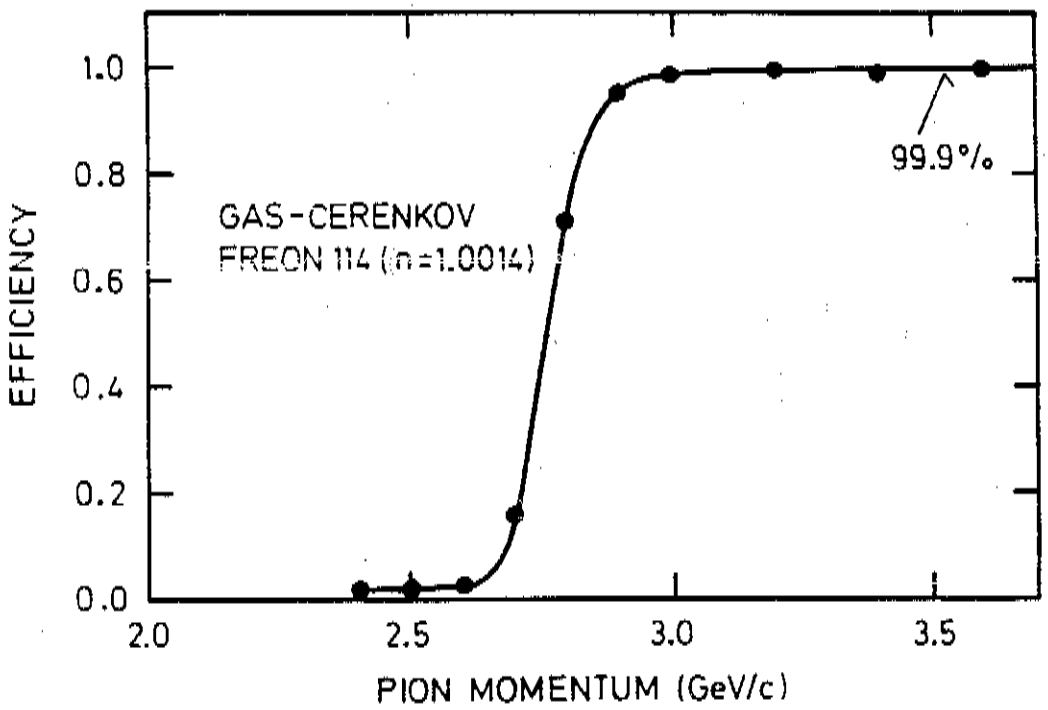
EFFICIENCY
1.0
0.8
0.6
0.4
0.2
0.0
GAS-CERENKOV
FREON 114 (n=1.0014)
99.9%
2.0
2.5
3.0
3.5
PION MOMENTUM (GeV/c)

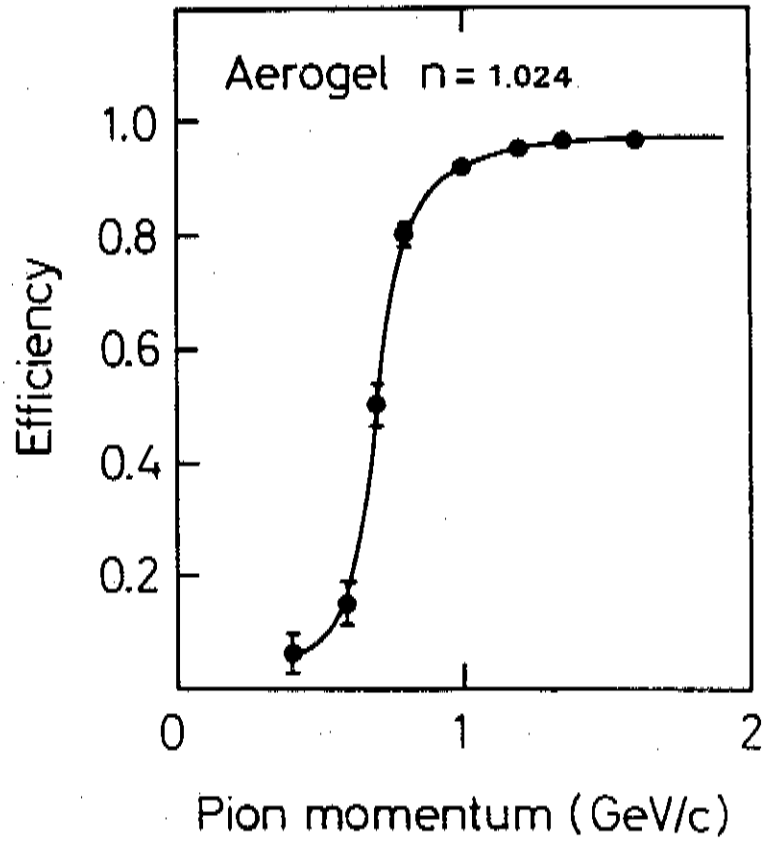
Aerogel n = 1.024
Efficiency
1.0
0.8
0.6
0.4
0.2
0
1
2
Pion momentum (GeV/c)

Differential Cerenkov Counter

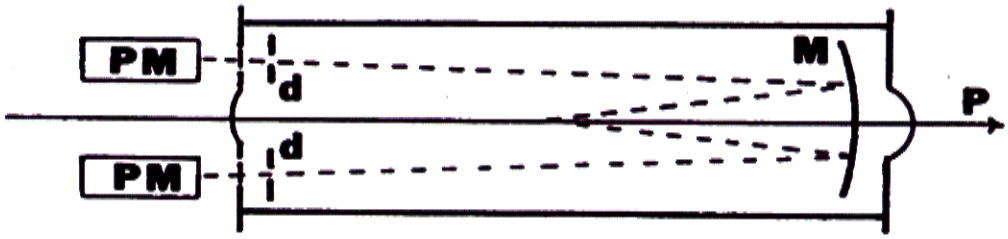

Differential

Spherical mirror with radius of curvature R and circular slit of radius $f\ tan\ \Theta_{det}$ at the focal plane, which is at $R/2$.

As gas pressure is increased, first π Cerenkov ring appears at $\simeq 0^o$, then moves out to higher angles. Next K ring appears at $\simeq 0^o$, and both π and K rings move out to higher angles. Then p threshold is reached, etc. When Θ_c for a particle type reaches Θ_{det}, its Cerenkov light is detected in the PMT's.

Resolution is limited by dispersion $\Rightarrow$ use a non-dispersive gas like He.

$$\Delta\Theta = \frac{\Delta n}{n\ tan\ \Theta}$$

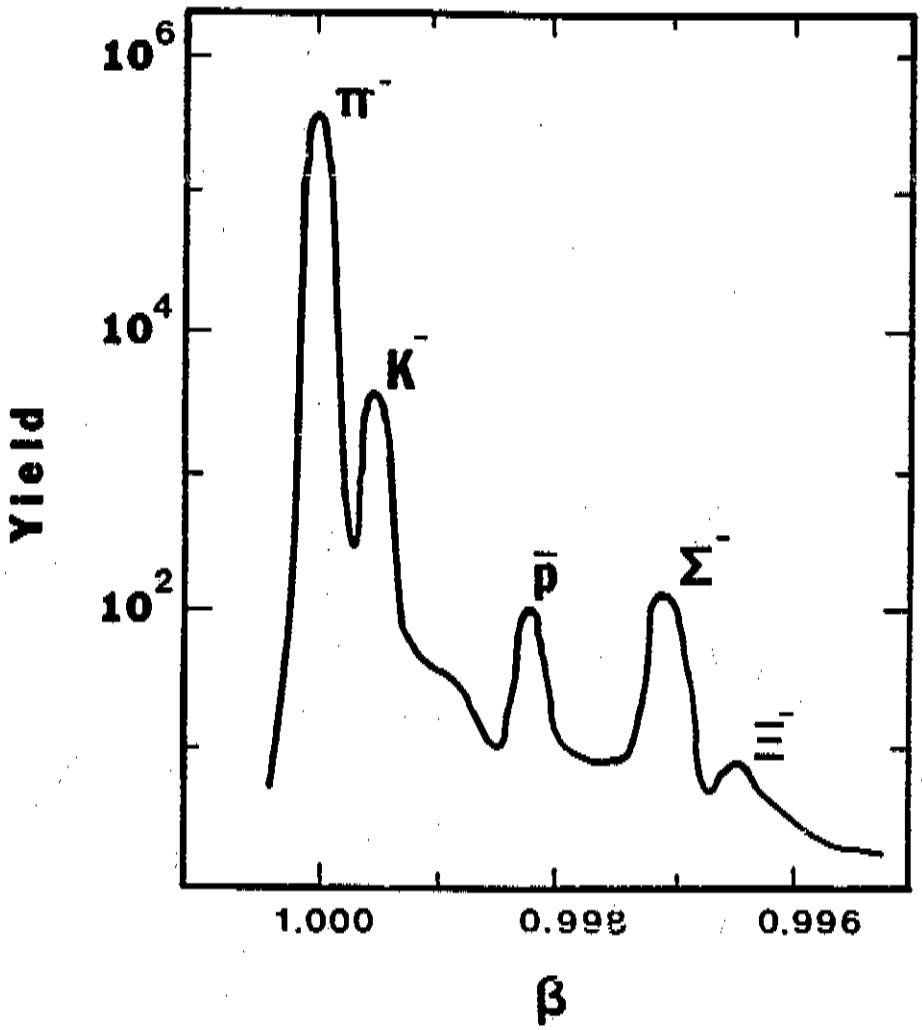

For a differential Cerenkov counter,

$$\frac{\Delta\beta}{\beta} = \tan\Theta\Delta\Theta$$

=> want <u>small</u> Θ and $\Delta\Theta$ for good velocity (i.e., mass) resolution.

But, Nphotons grows with Θ and $\Delta\Theta$, so the counter will be inefficient if they are too small. With careful tuning, resolution of 10^{-7} in $\Delta\beta$ has been achieved.

Ring Imaging Cerenkov Counter

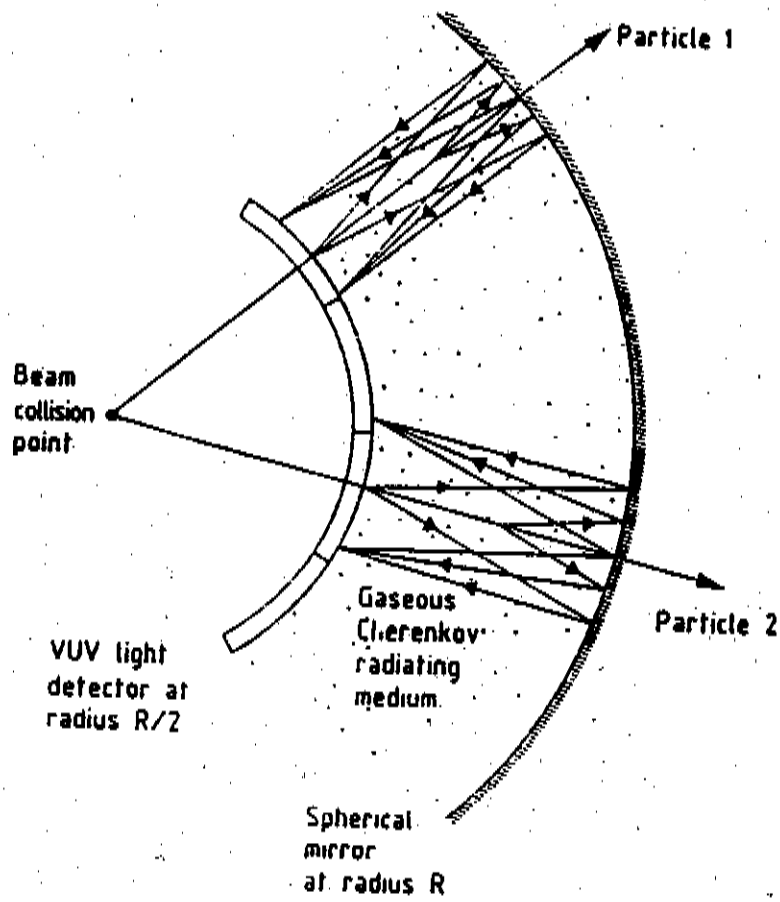

(As first proposed by Ypsilantis and Seguinot) Spherical mirror with radius of curvature R centered at interaction point with detector at the focal plane, which is at $R/2$.

Ring radius identifies particle type. Various species can be identified in the same detector.

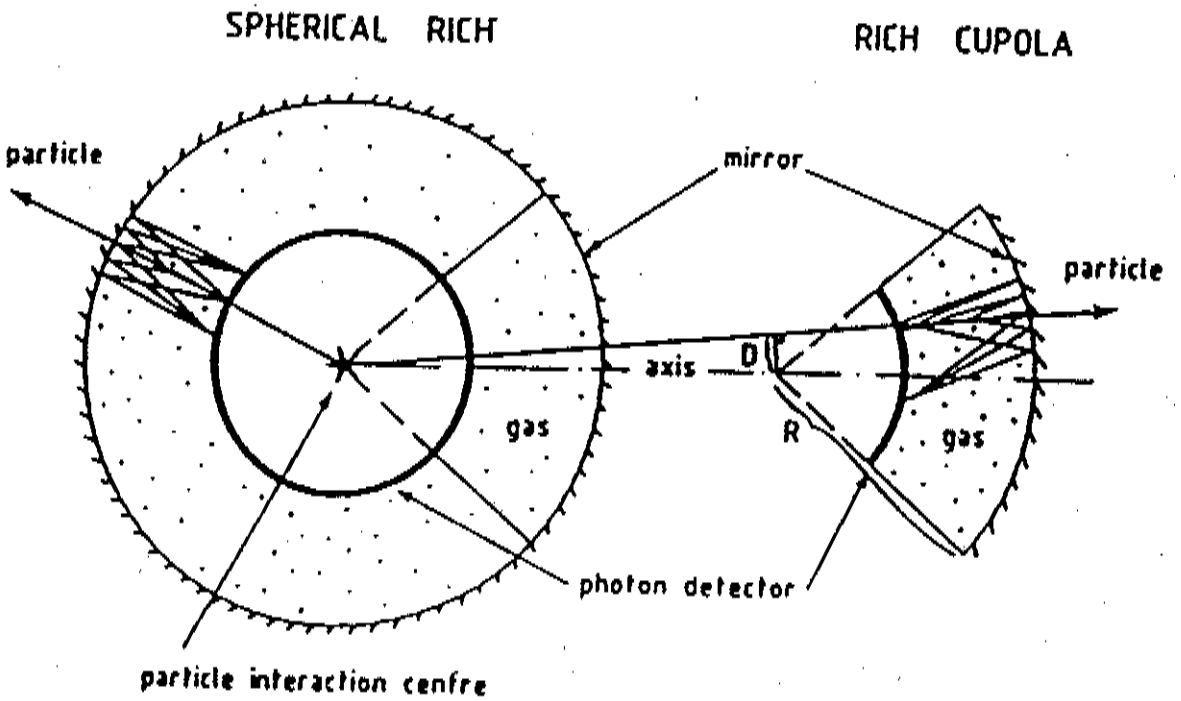
SPHERICAL RICH
RICH CUPOLA
particle
mirror
particle
axis
D
gas
R
gas
photon detector
particle interaction centre

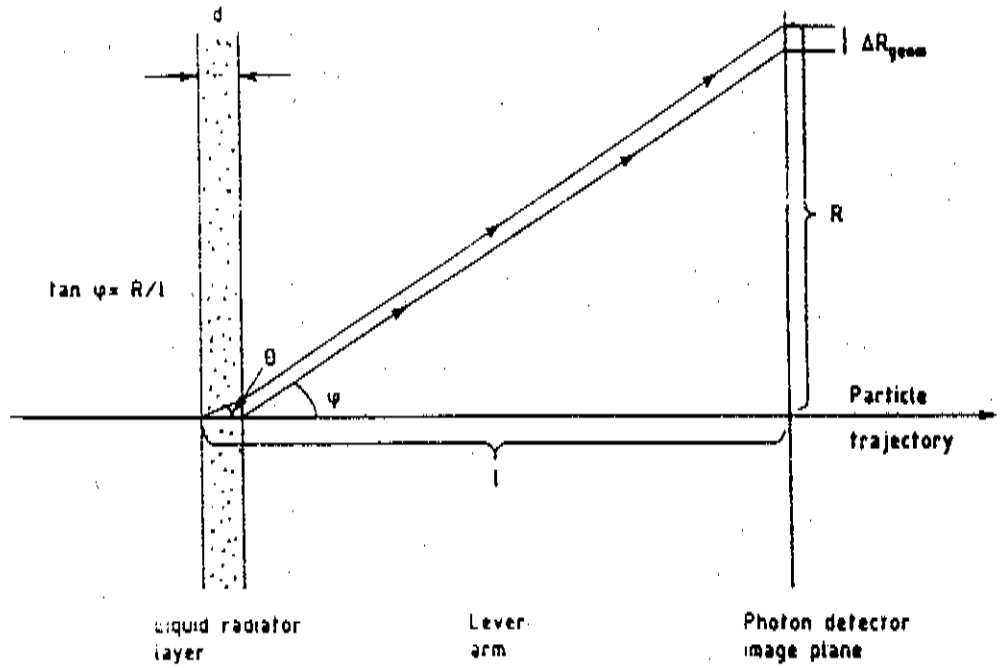

PROXIMITY FOCUSING

RESOLUTION GOES AS $\frac{\Delta R}{R}$

SINCE RAYS ARE PARALLEL ΔR DOES

NOT GROW WITH L

R DOES INCREASE LINEARLY WITH L

LIQUID RADIATOR (C_6F_{14})

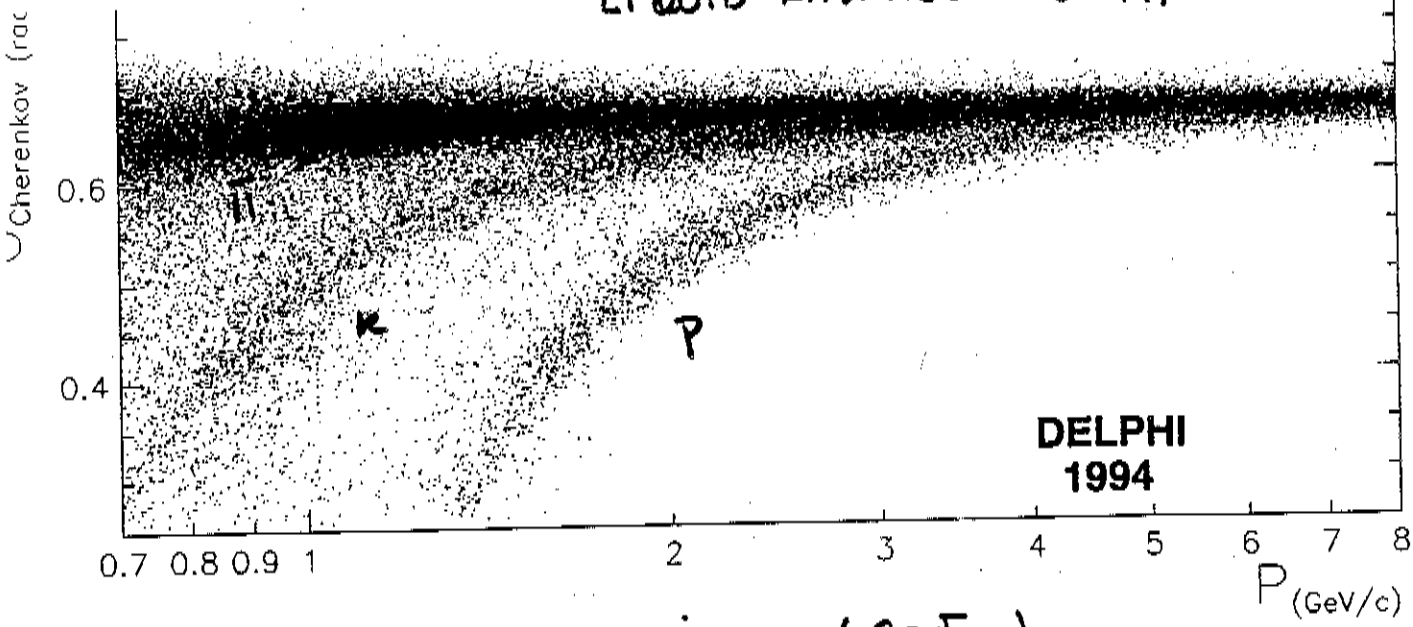

GAS RADIATOR (C_5F_{12})

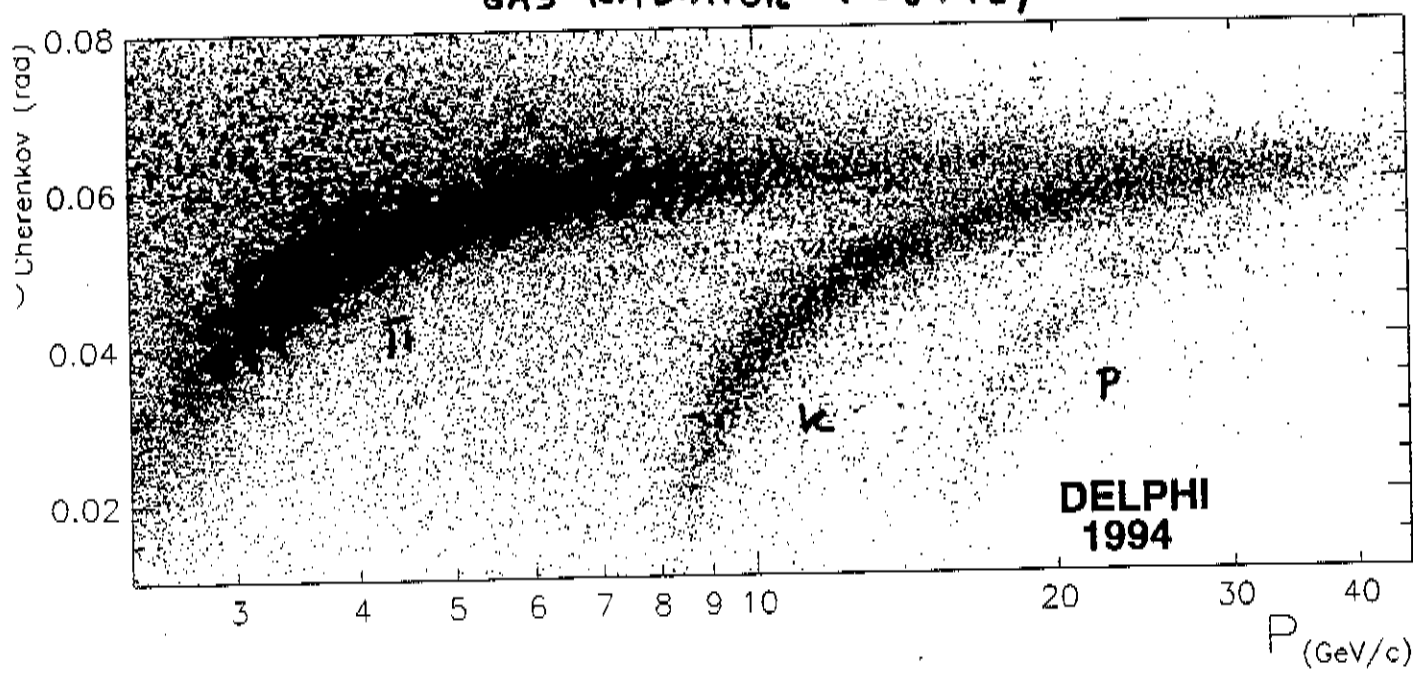

RICH

GAS / LIQUID

PERFLOR CARBON

$$\cos\theta_c = \frac{1}{n\sqrt{1+m^2/p^2}}$$

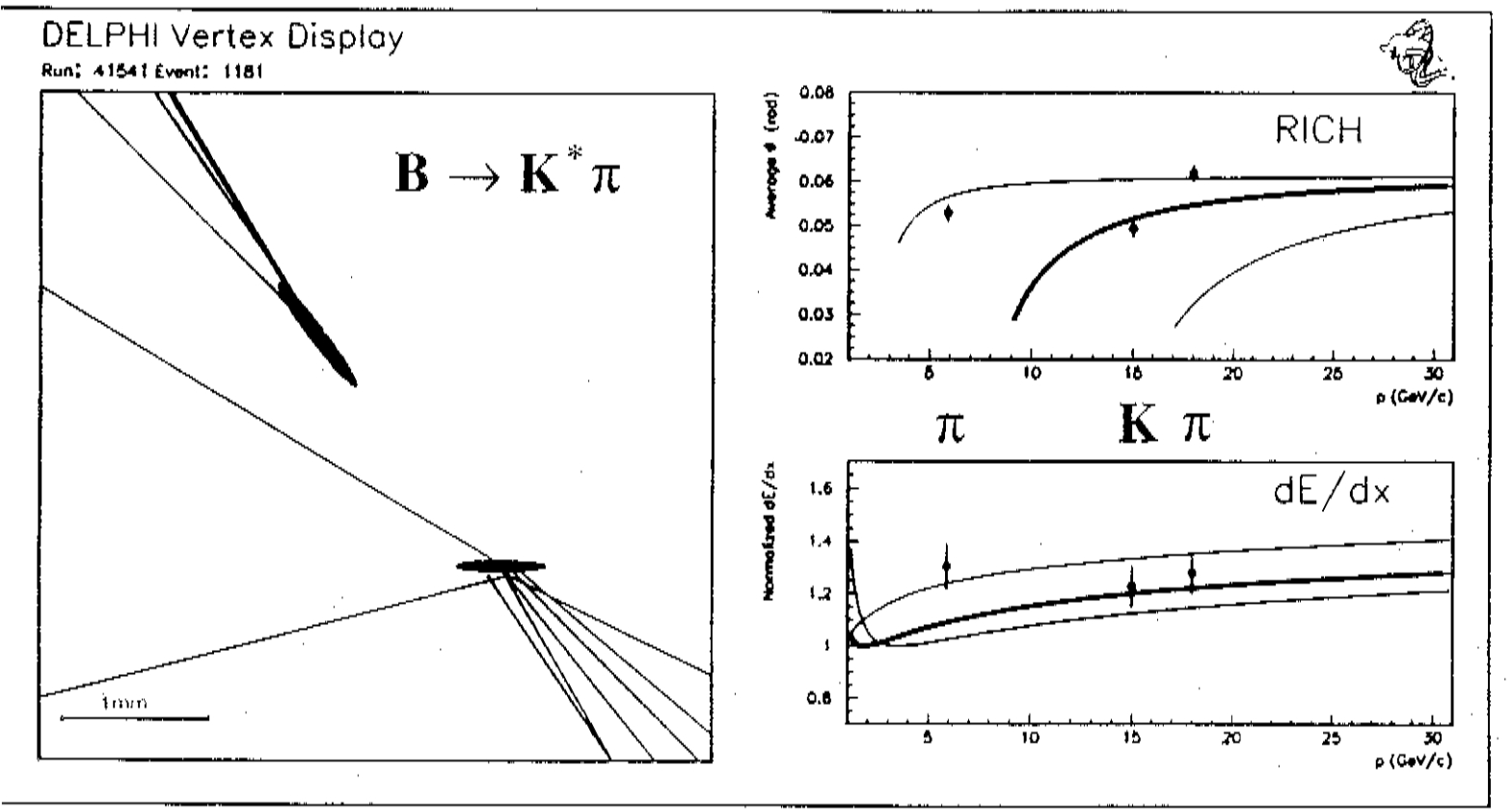
DELPHI Vertex Display
Run: 41541 Event: 1181
B → K* π
1mm
RICH
Average θ (rad)
p (GeV/c)
π K π
dE/dx
Normalised dE/dx
p (GeV/c)

ISOLATED KAON

P = 10.60 GeV/c

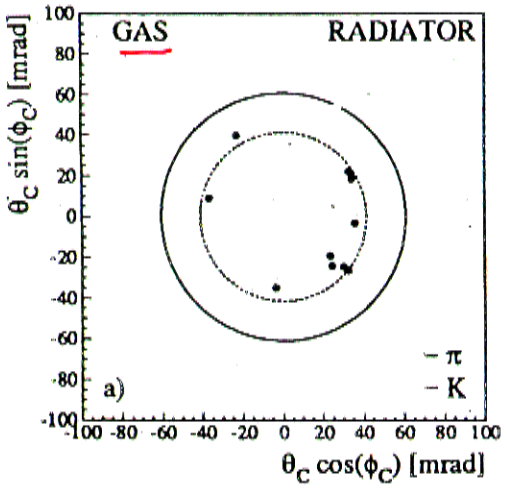

PION IN JET

P = 0.86 GeV/c

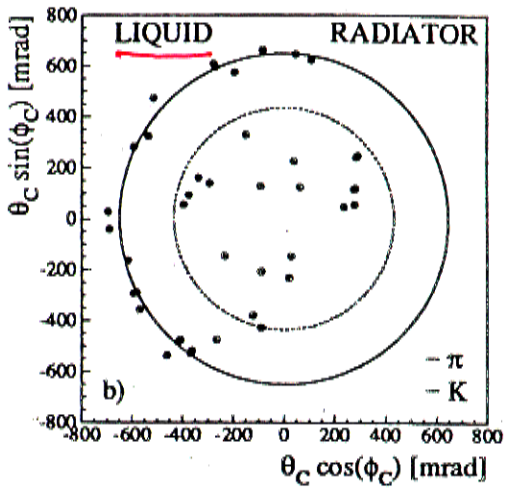

VETO FOR K, p BELOW THRESHOLD FOR K

π/K/p UP TO ~ 20 GeV/c

K/p UP TO ~ 25 GeV/c

π/K/p separation up to 4.5 GeV/c

K/p sep up to ~ 6 GeV/c

SOPHISTICATED MAXIMUM LIKELIHOOD TECHNIQUES

USE BOTH # OF PHOTONS AND MEAN RING RADIUS OF HITS

(14)
17.

$\phi(1020) \to K^+K^-$

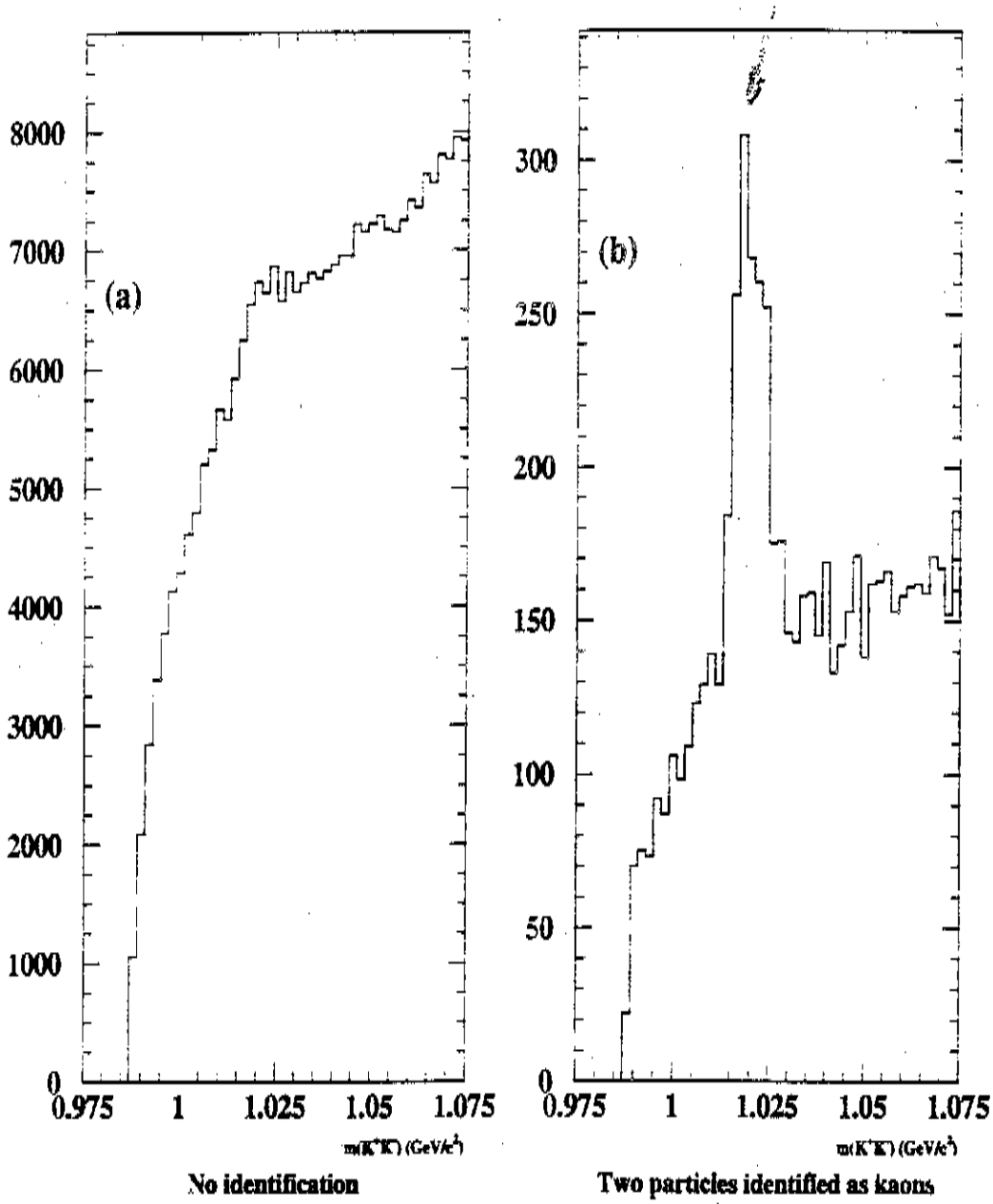

Figure 2: K^+, K^- invariant mass distribution after kinematical cuts obtained (a) before and (b) after kaon identification.

DETECTOR IS TYPICALLY A WIRE CHAMBER FILLED WITH A GAS THAT CONTAINS TMAE OR TEA (PHOTOSENSITIVE)

WIRES FOR ONE DIMENSION
PADS ON BACK OF RESISTIVE CATHODE FOR THE OTHER.

OR, FOR CASES WHERE LONG DRIFT TIMES CAN BE ACCOMODATED, A TIME PROJECTION CHAMBER (TPC)

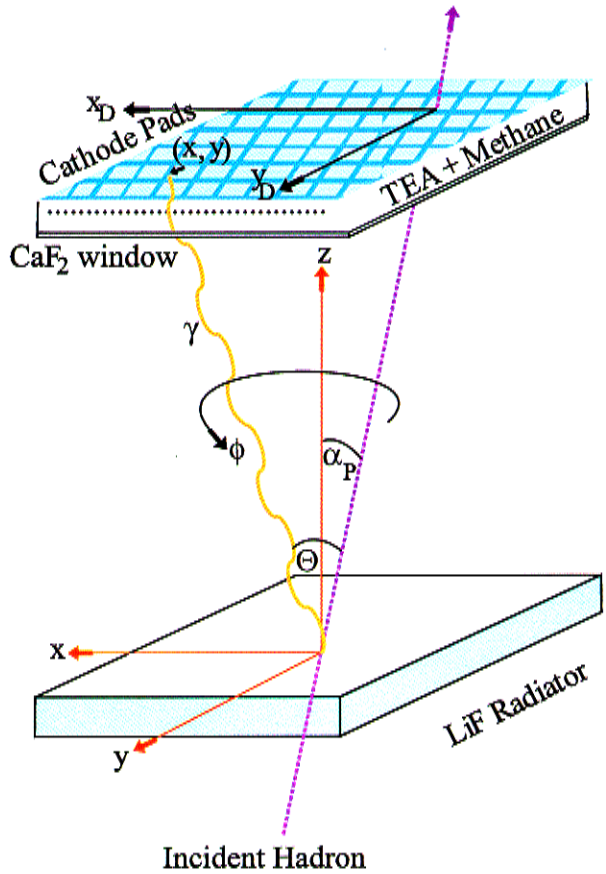

Fig. 2. Schematic diagram of LiF-TEA RICH system.

light (UV) transparent N_2 gas.

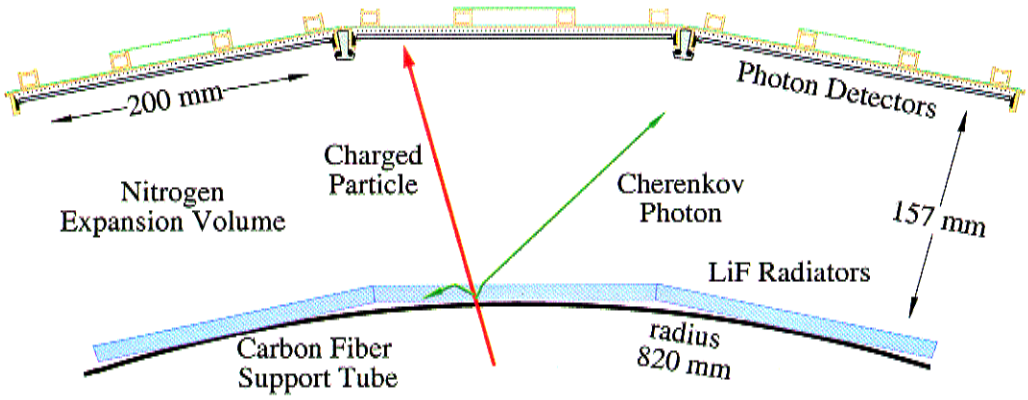

Fig. 3. A section of one tenth of the RICH detector as seen from the end.

A sketch of a photon detector module is shown in Fig. 4. The wires run the entire length of the detector, approximately 2.5 m. They are supported every 30 cm by a ceramic spacer. The CaF_2 window joints are placed directly on top of these spacers to minimize the loss of photon acceptance. Some parameters of the RICH detector are given in Table 1.

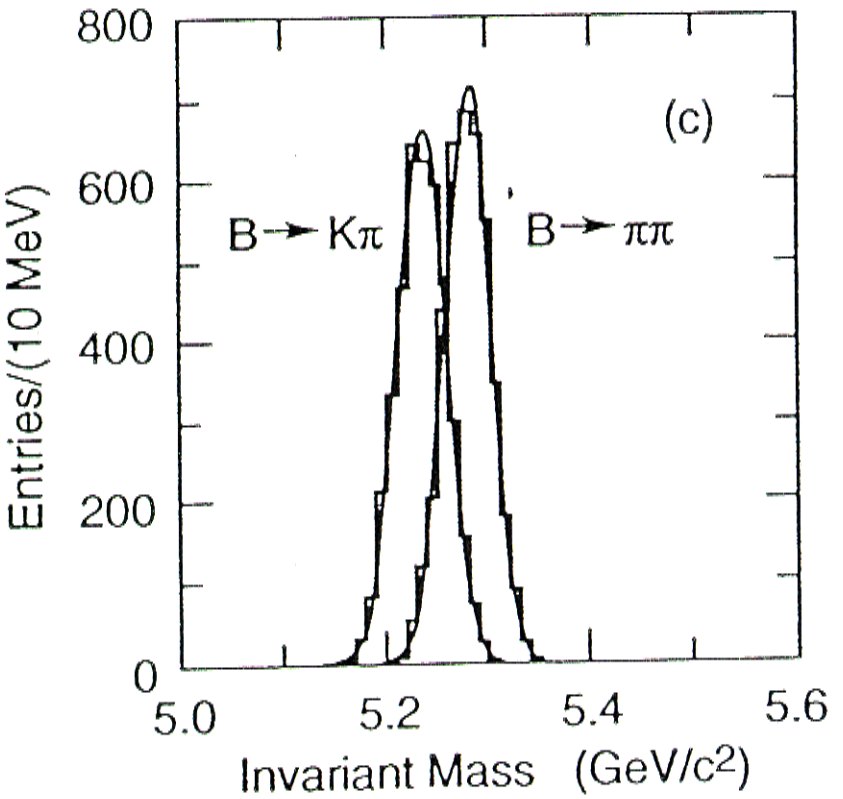

$$\frac{\sigma_{p_T}}{p_T^2} = .23 \left(\frac{GeV}{c}\right)^{-1}$$

ASSUMED

But, some B decays of special importance have π's and K's of higher momenta - $p_\pi \gtrsim 2$ GeV/c for $B^0 \to \pi^+\pi^-$, e.g. - measure $|V_{ub}|$

- if tagged, see CP violation

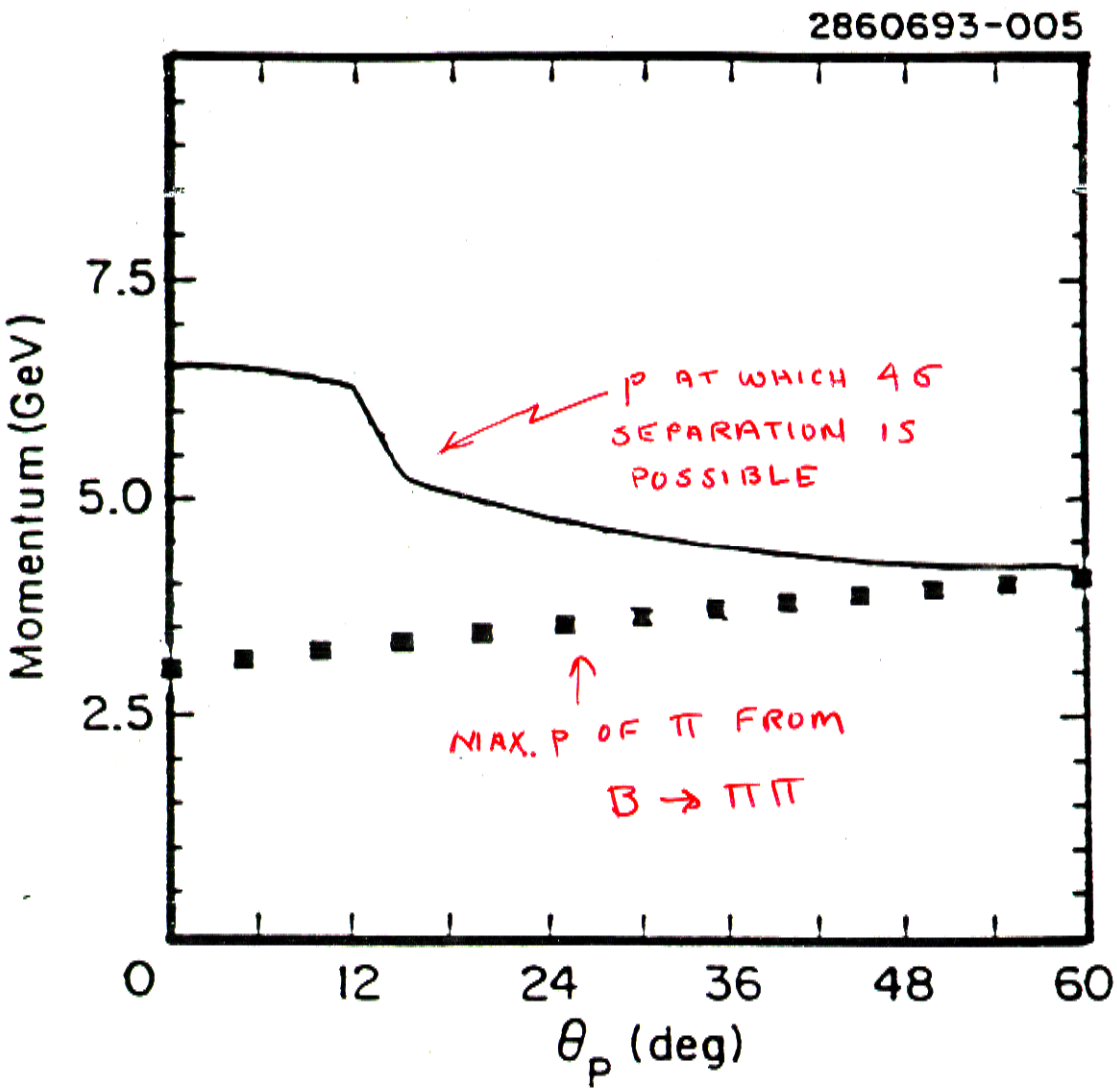

RICH PROPOSED FOR CLEO UPGRADE

NA44 Pb – Pb COLLISIONS

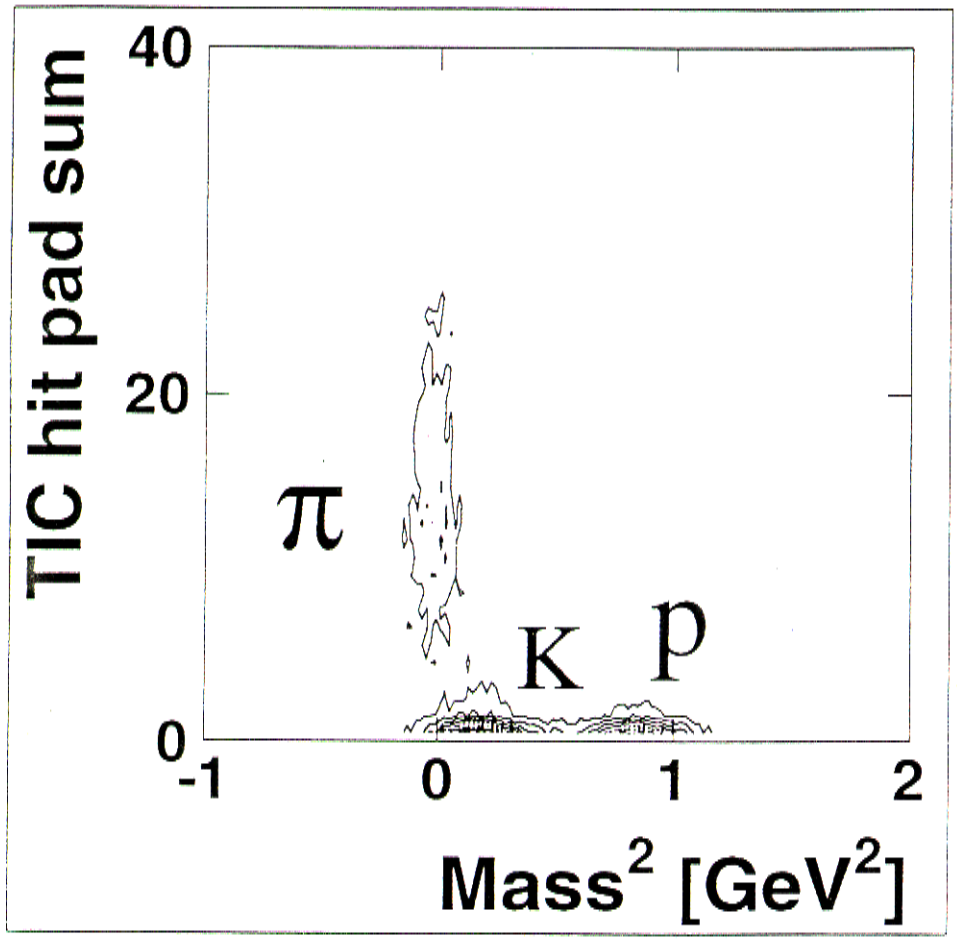

$3 < p < 8$ GeV/c

TIC (Threshold Imaging Cherenkov) Detector

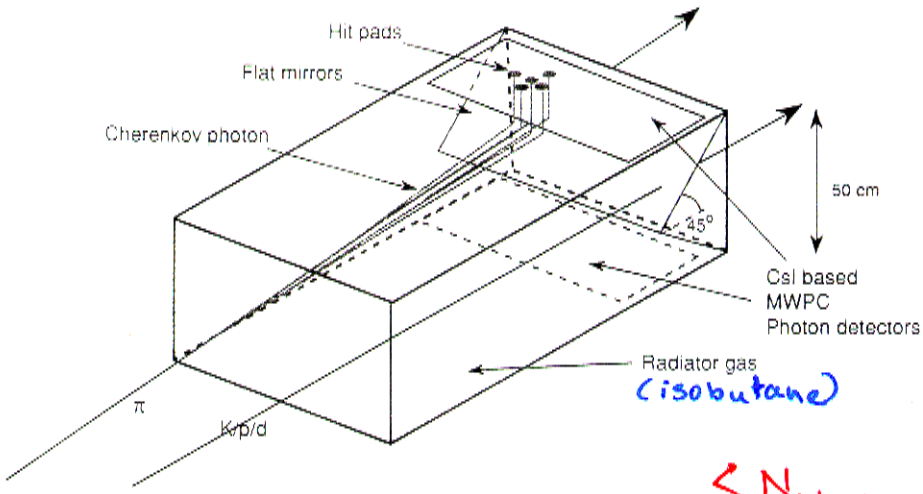

Schematic view of the detector

$\langle N_{photons} \rangle \sim 15$ for π's

CsI Cathode

DIRC

Detection of Internally Reflected Cerenkov Light

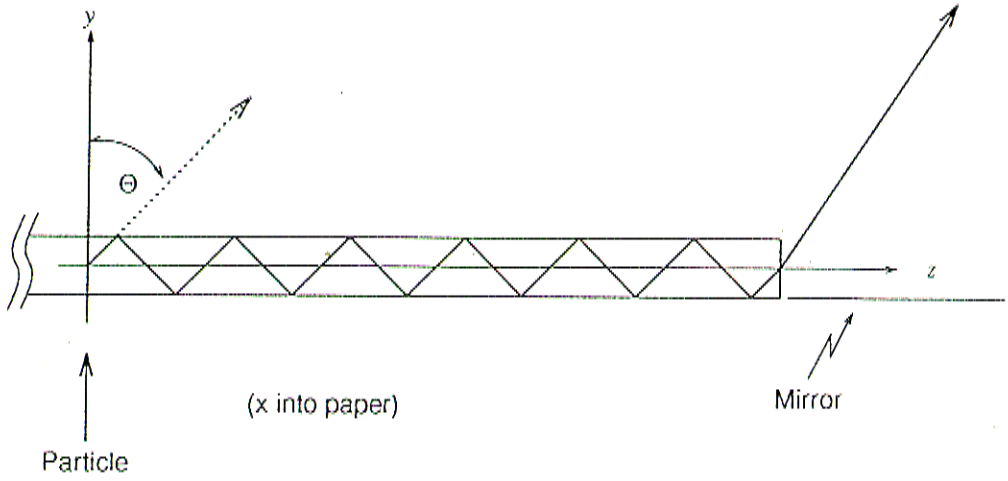

Figure 5.18: Propagation of light trapped by total internal reflection in the quartz bars of the DIRC.

initial photon momentum vector

$$\vec{p} = (p_x, p_y, p_z)$$

final photon momentum vector

$$\vec{p}\,' = (p_x', p_y', p_z')$$

where $p_x' = (-1)^n p_x \quad p_y' = (-1)^m p_y$

$$p_z' = p_z$$

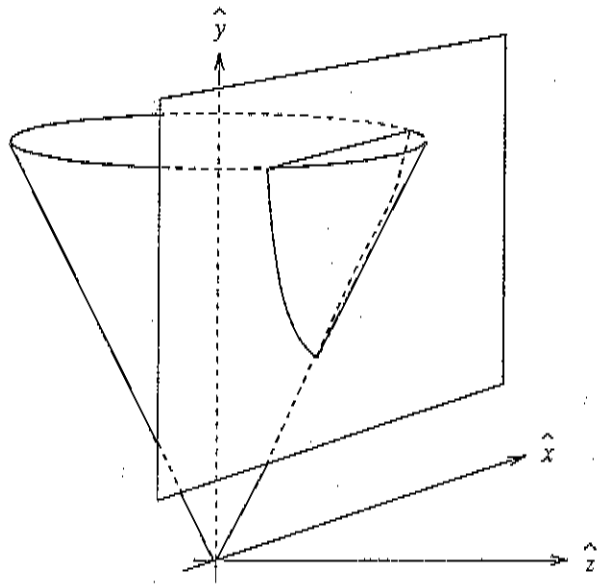

Figure 5.19: Image formation for a DIRC. In the ideal case considered the image is a hyperbola.

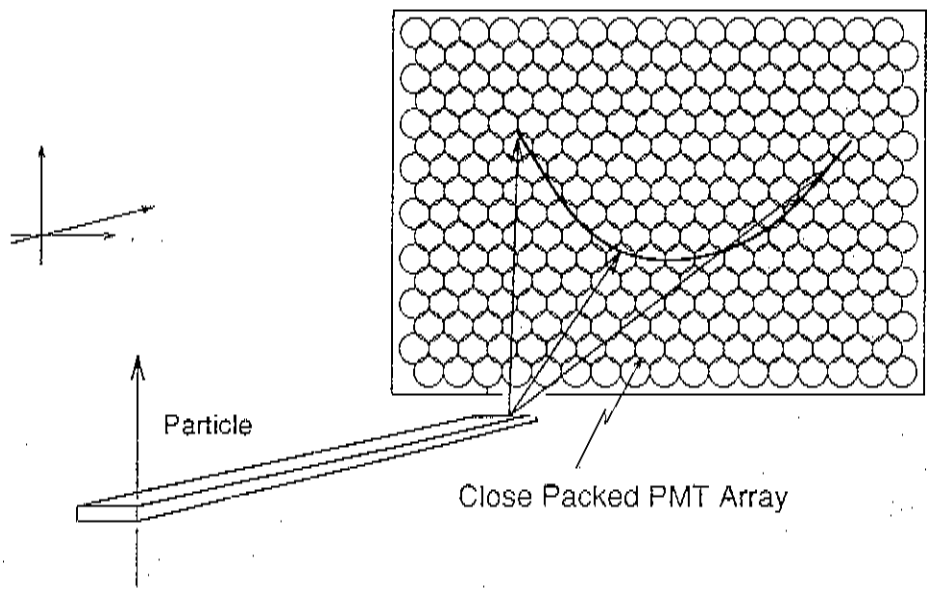

Figure 5.20: Schematic view of DIRC image formation.

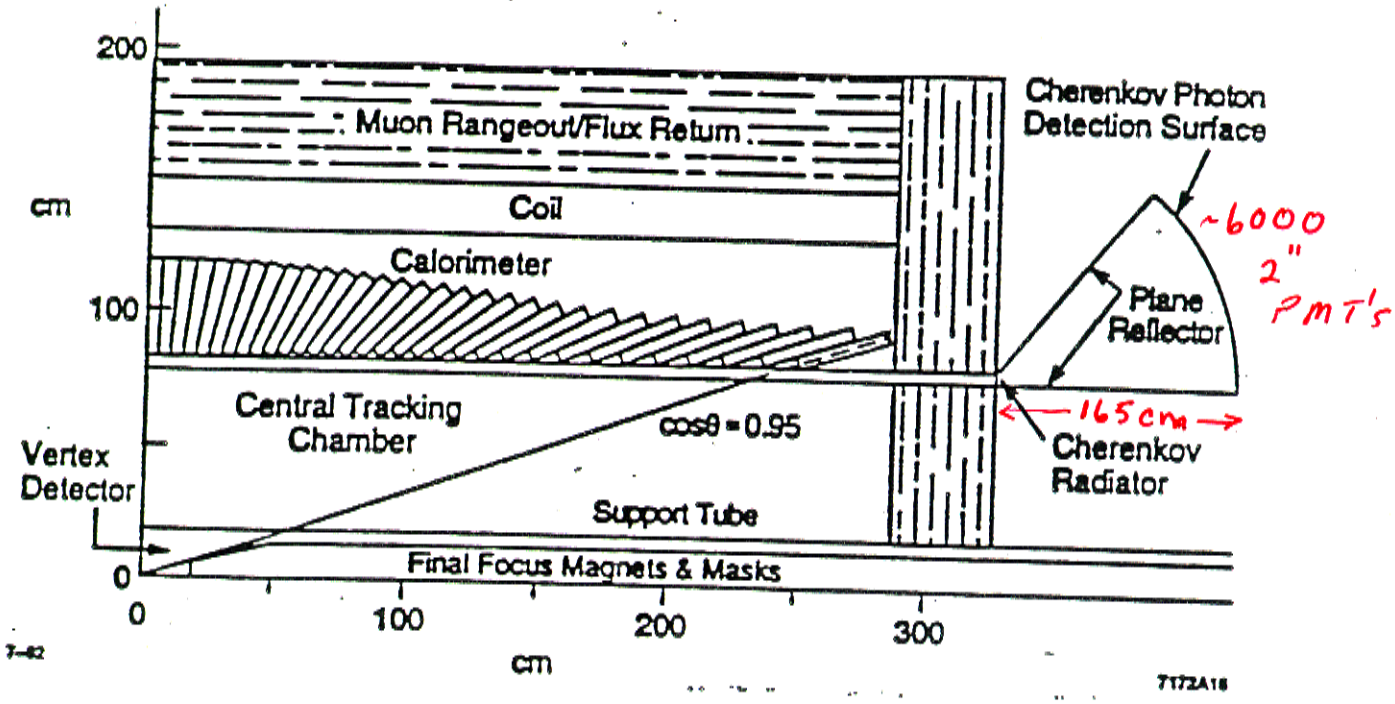

Schematic view of one quadrant of a B factory detector incorporating a DIRC and without an endcap calorimeter.

DIRC

125 quartz bars

1.2 cm thick (in y)

4 cm wide (in x)

260 cm long from center to end

$n = 1.474$ $\theta_c = 47.3$ for $\beta = 1$

The DIRC

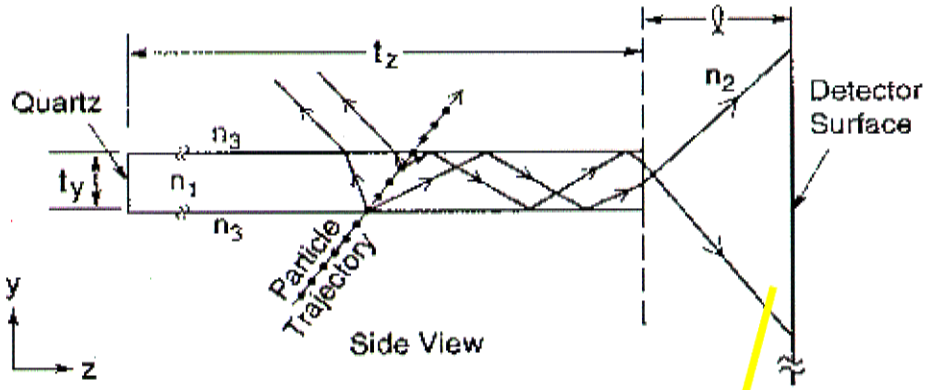

Measured in Dch

$$p = m\,\beta\gamma$$

Measured in DIRC

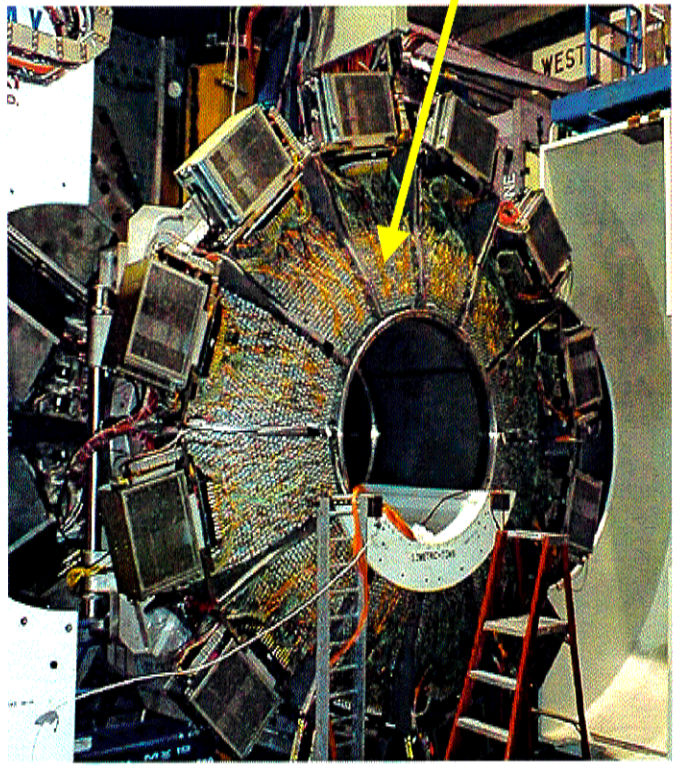

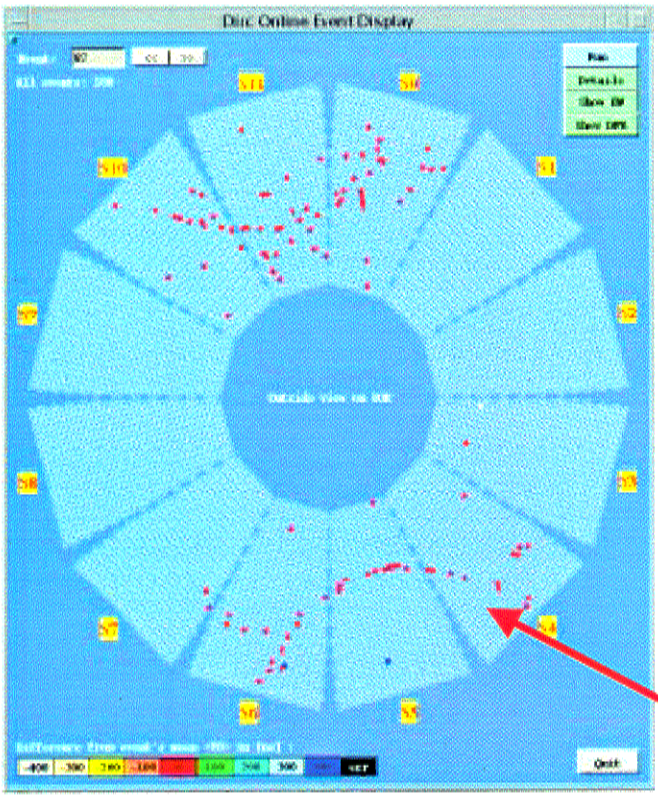

Cherenkov Ring

DIRC Performance

$D^{*+} \rightarrow D^0 \pi^+$
$\hookrightarrow K^- \pi^+$

- Kinematically select sample of K/π

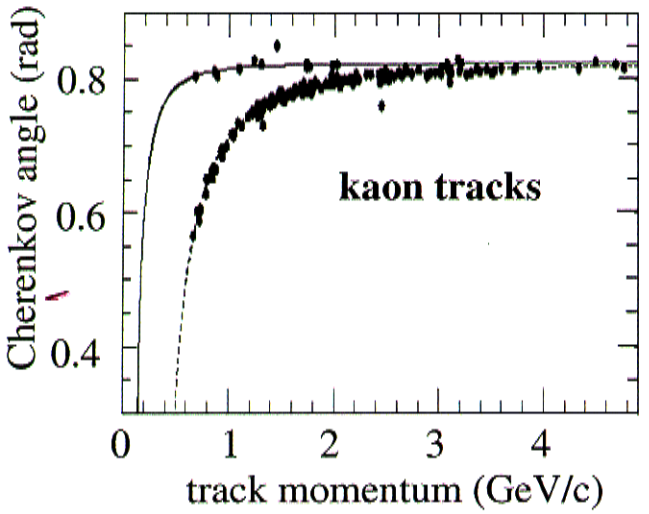

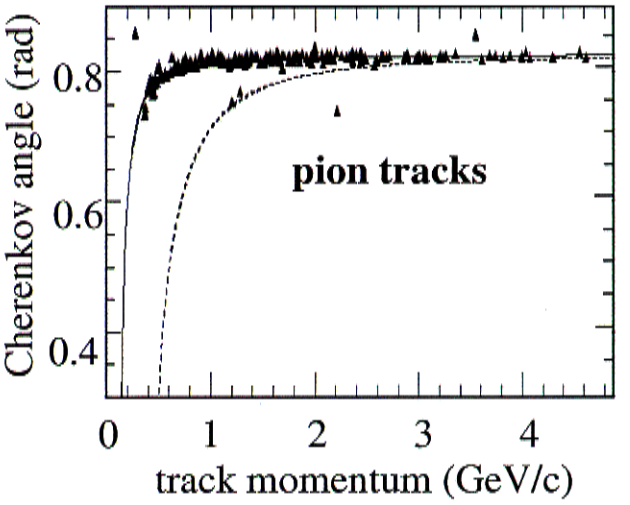

$D^0 \rightarrow K^- \pi^+$

- $p^*(D^0) > 1.5$ GeV/c; $0.5 < p(K) < 4.0$ GeV/c

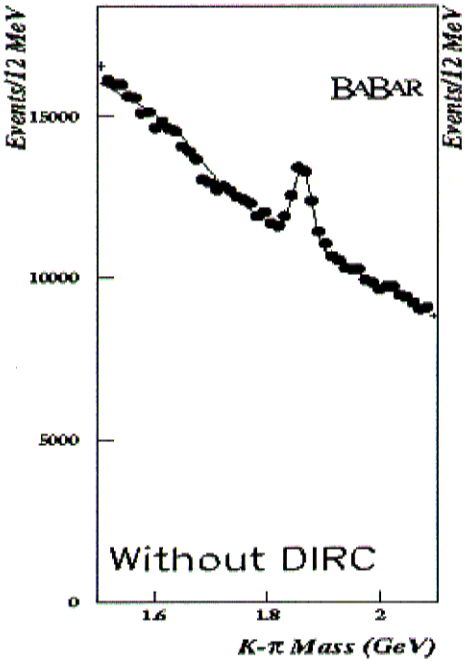

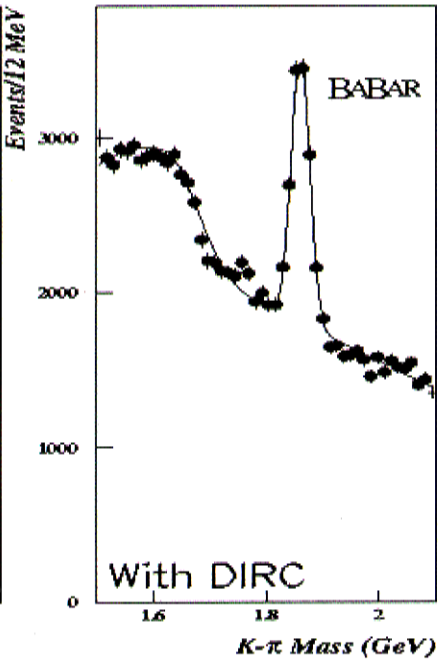

- K efficiency within DIRC acceptance ~80%
- Background to D^0 reduced by factor ~5.

dE/dx Performance

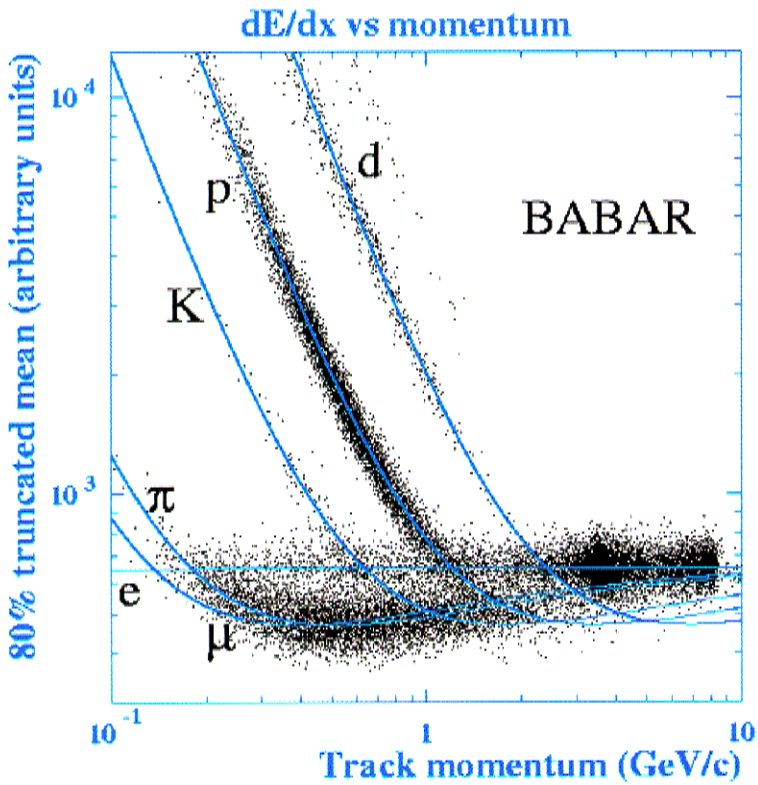

Drift Chamber

- 7.5% resolution for Bhabhas
- > 3σ K/π separation up to ~700 MeV

Silicon Vertex Detector

- 17% resolution for MIPS
- 2σ K/π separation up to ~500 MeV

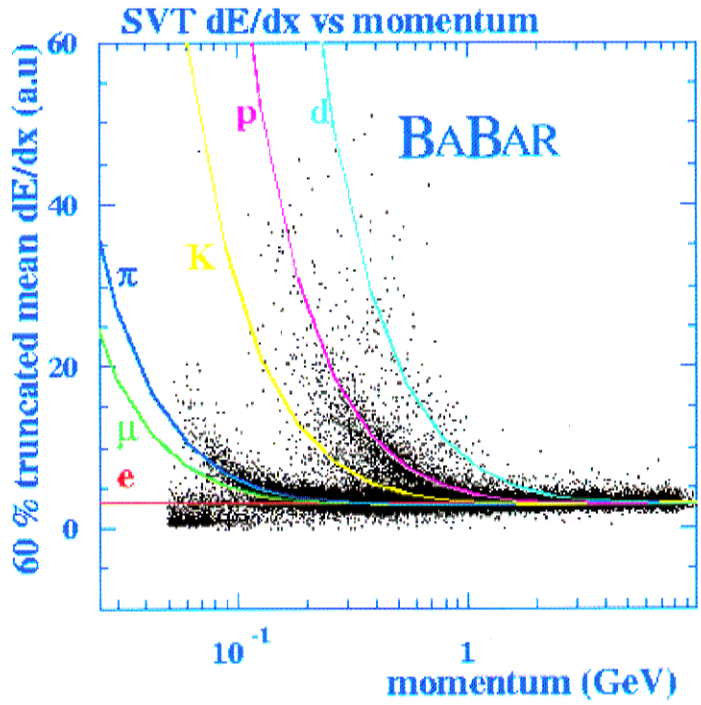

TRANSITION RADIATION

is the radiation that <u>must be emitted</u> as a relativistic particle crosses the interface between two materials with different dielectric constants. Like Cerenkov radiation, this is a bulk property of matter.

Like Cerenkov Radiation,
Transition Radiation ...

- was first predicted by Russian physicists
  Ginzburg and Frank - mid 1940's

- is a <u>relativistic</u> effect
  particle velocity > velocity of light

- is a <u>bulk</u> effect
  foil thickness $\geq$ "formation zone"

- is a <u>small</u> effect
  $\sim \alpha$, the fine structure constant

For a single interface, an approximate expression for the energy radiated per unit solid angle per unit frequency interval is

$$\frac{d^2W}{d\omega d\Omega} = \frac{\alpha}{\pi^2}\left|\frac{\Theta}{\gamma^{-2}+\Theta^2+\frac{\omega_{p1}^2}{\omega^2}} - \frac{\Theta}{\gamma^{-2}+\Theta^2+\frac{\omega_{p2}^2}{\omega^2}}\right|^2$$

assuming $\gamma \gg 1$, $\Theta \ll 1$, and $\omega^2 \gg \omega_{p1}^2, \omega_{p2}^2$.

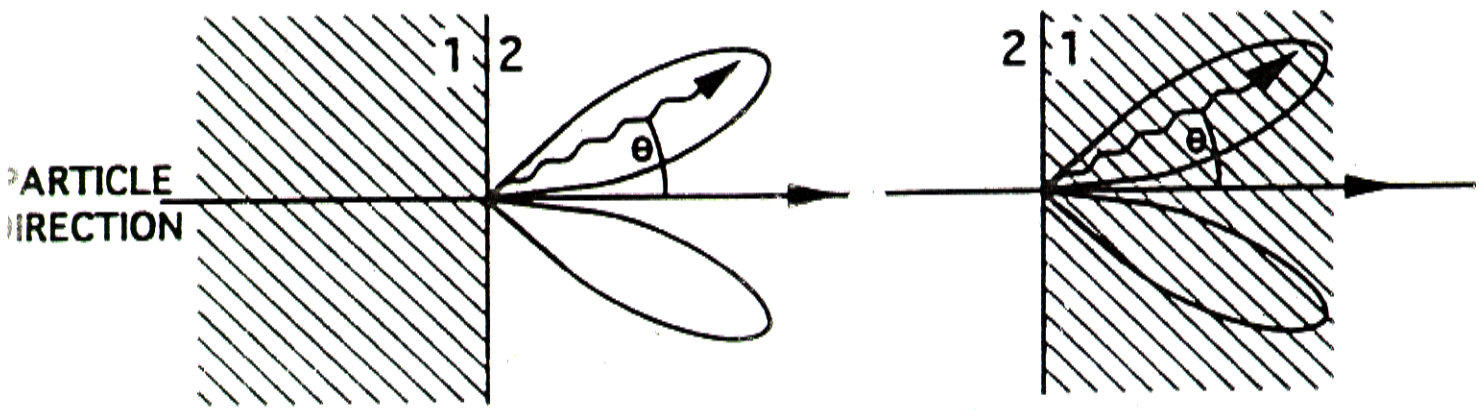

Notice that the radiation is

- Strongly peaked in the forward direction
- Symmetric
- Larger for larger differences in the plasma frequencies

e.g. $\begin{cases} CH_2 \text{ foils } 21\,eV \\ \text{Air gaps } 0.7\,eV \end{cases}$

For a single foil in a gas, the amplitude of the transition radiation measured at the point where the particle exits the foil is:

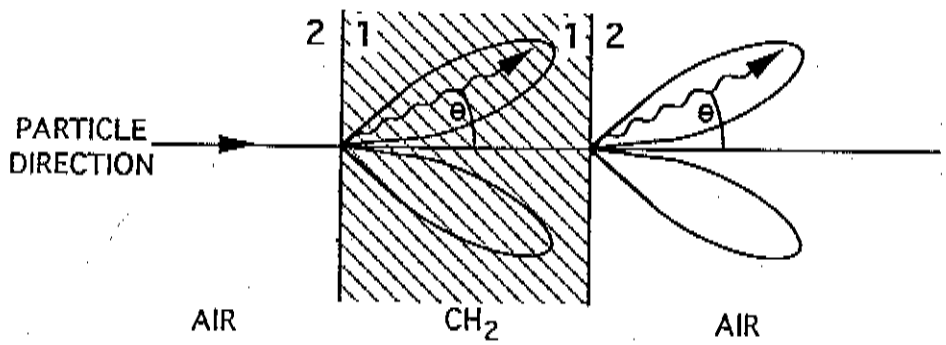

$$\vec{E}(\omega, \vec{\Theta}) = \vec{e_2}(\omega, \vec{\Theta}) + \vec{e_1}(\omega, \vec{\Theta})e^{-(\sigma + i\phi)},$$

where $\vec{e_i}(\omega, \vec{\Theta})$ is the amplitude of the radiation at surface i, σ is the attenuation in the foil, and ϕ is the phase lag due to the difference in the velocities of the particle and light in the medium.

Neglecting attenuation, which is a very small effect for a single foil,

$$\vec{e_1}(\omega, \vec{\Theta}) = \frac{\vec{\Theta}}{\gamma^{-2} + \Theta^2 + \frac{\omega_{p,air}^2}{\omega^2}} - \frac{\vec{\Theta}}{\gamma^{-2} + \Theta^2 + \frac{\omega_{p,foil}^2}{\omega^2}}$$

$$= -\vec{e_2}(\omega, \vec{\Theta})$$

Then, squaring to get the intensity of the radiation, we see that the transition radiation from a single foil is the same as that from a single interface modulated by a factor that depends on the phase lag

$$\left(\frac{d^2W}{d\omega d\Omega}\right)_{foil} = \left(\frac{d^2W}{d\omega d\Omega}\right)_{interface} \times 4sin^2\left(\frac{\phi}{2}\right)$$

and we get positive interference for $\phi = \pi, 3\pi, \ldots$.

It can be shown (Artru eqn 2.10) that

$$\phi_{foil} \simeq \frac{(\gamma^{-2} + \Theta^2 + \frac{\omega_{p,foil}^2}{\omega^2})\omega l_{foil}}{2},$$

where l_{foil} is the foil thickness.

If we define

$$z_{foil} \equiv \frac{2}{(\gamma^{-2} + \Theta^2 + \frac{\omega_{p,foil}^2}{\omega^2})\omega},$$

then $\phi_{foil} = \frac{l_{foil}}{z_{foil}}$.

z_{foil} is the well-known formation zone. If l_{foil} is much smaller than this, we get no transition radiation from the foil.

THIS IS A SMALL EFFECT - THE TOTAL ENERGY RADIATED AT A SINGLE INTERFACE IS OF ORDER $\alpha = \frac{1}{137}$.

BUT, BY STACKING MANY (~ 200) FOILS OF MATERIAL 1, SEPARATED BY GAPS OF MATERIAL 2, AND CHOOSING THE FOIL THICKNESS TO GET POSITIVE INTERFERENCE BETWEEN THE RADIATION EMITTED AT THE INCIDENT AND EXIT SURFACES, IT IS POSSIBLE TO ENHANCE THE EFFECT ENOUGH TO BUILD A PRACTICAL DETECTOR.

THIS PROCEDURE CAN BE GENERALIZED TO AN N-FOIL RADIATOR BY GROUPING THE AMPLITUDES 2 × 2 AND ADDING THEM COHERENTLY. IT IS POSSIBLE TO MAKE A SERIES APPROXIMATION TO THE EXPRESSION THAT RESULTS. THE INTEGRATION OVER Θ IS PERFORMED BECAUSE THE ANGLES ARE SO SMALL THAT THE DETECTORS BUILT TO DATE SEE THE RADIATION IN THE SAME CELL AS THE PARTICLE TRACK (THE TRACK COULD BE BENT AWAY BY USE OF A MAGNETIC FIELD, HOWEVER)

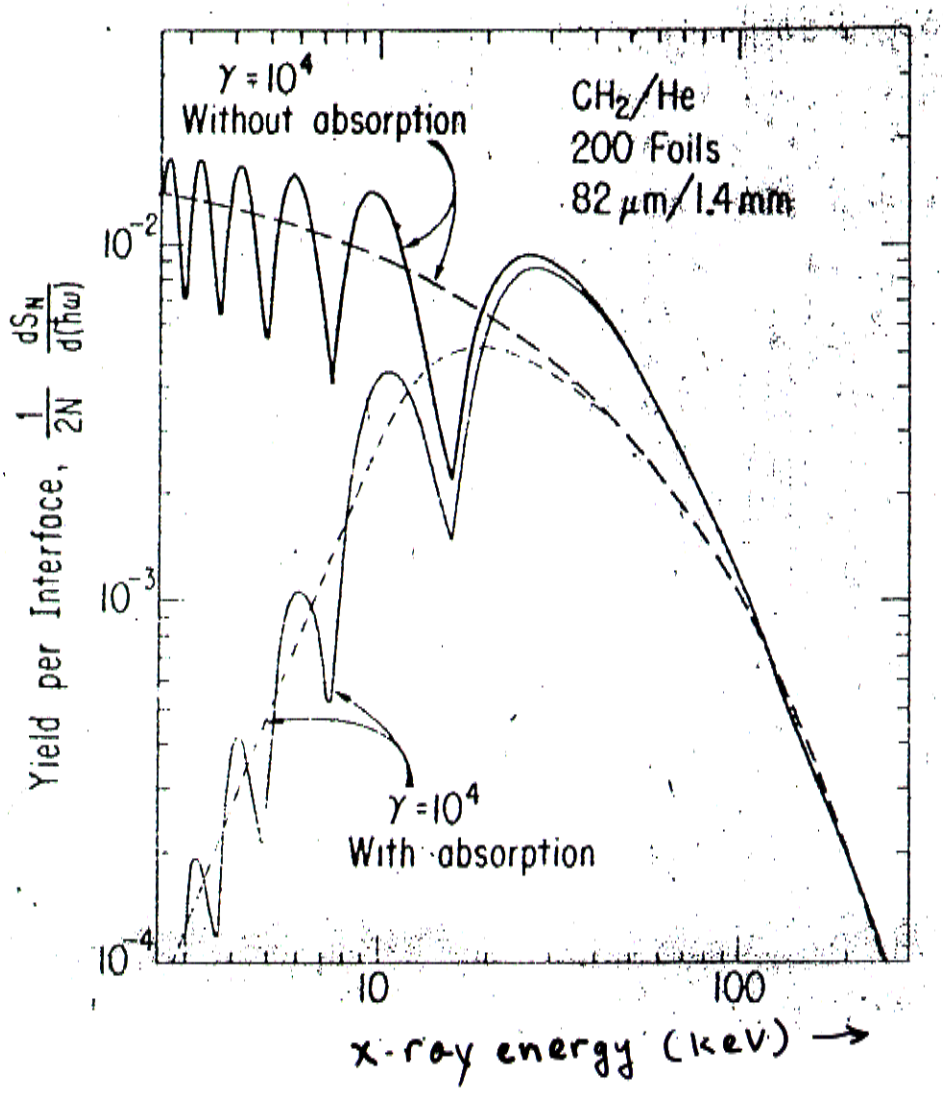

FROM p. 2248 OF CHERRY'S PRD ARTICLE, FOR 200 CH_2 FOILS, 82 μm THICK, WITH 1.4 mm He GAPS, $\gamma = 10^4$

TOTAL YIELD FROM 200 FOILS IS 400 TIMES THE YIELD/INTERFACE, WHICH IS WHAT IS SHOWN ON THE PLOT VS X-RAY ENERGY

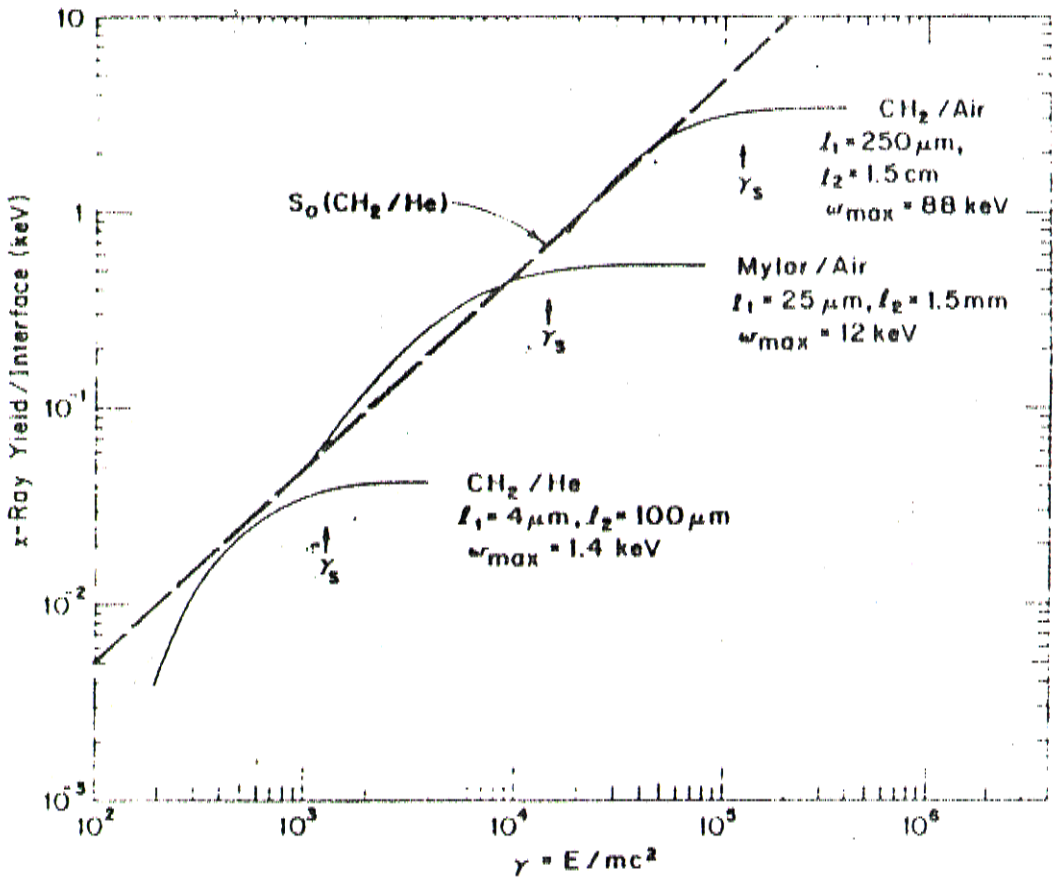

FIG. 2. Total energy radiated per interface in the absence of absorption for a single CH_2/He interface (dashed line) and for three different many-foil radiators (solid lines), as a function of Lorentz factor. Arrows mark the saturation energies γ_S predicted from Eq. (14c).

$$\gamma_{SAT} \simeq \gamma_{SAT}(\omega_{max}) \simeq 0.6\, \omega_1 (l_1 l_2)^{1/2}/c$$

INCREASES WITH BOTH l_1 AND l_2

E769

USED FOR PI VERSUS K OR P $\gamma_\pi \sim 1800$

IDENTIFICATION IN A

250 GEV HADRON BEAM

AT RATES UP TO 2 MHZ

(AND SOMETIMES EVEN HIGHER)

EXPERIMENTAL GOAL WAS TO

RECORD DATA SETS OF NEARLY

EQUAL STATISTICAL SIGNIFICANCE

FOR EACH INCIDENT PARTICLE TYPE

TO STUDY THE BEAM FLAVOR

DEPENDENCE OF CHARM

HADROPRODUCTION

OVERALL DESIGN FEATURES

HIGH RATES ⇒ THIN CHAMBER GAPS 6.35 mm

NARROW WIRE SPACING 1 mm

$\sigma_{BEAM} \sim .8$ cm – 68% OF BEAM

SHINES ON ~ 16 WIRES. THIS MEANS

THAT THE HOTTEST WIRES SEE

$\sim 4.25 \times 10^4$ PARTICLES/SEC ALONG $\gtrsim$ 2 cm

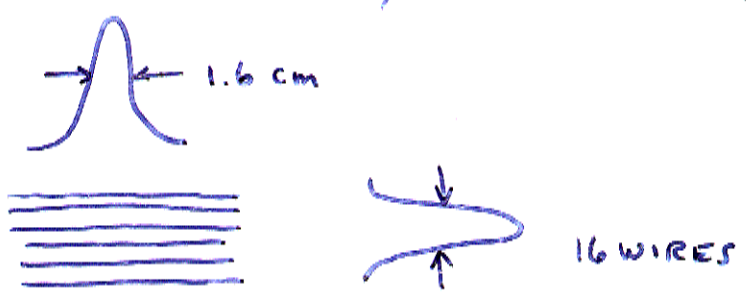

THIS PUSHES THE SAULI LIMIT OF

$\sim 3 \times 10^4$ / SEC / cm

WE BELIEVE WE DO SEE SPACE CHARGE

EFFECTS AT $\gtrsim$ 2 MHz BUT NOT

ENOUGH TO SEVERELY COMPROMISE TRD PERFORMANCE

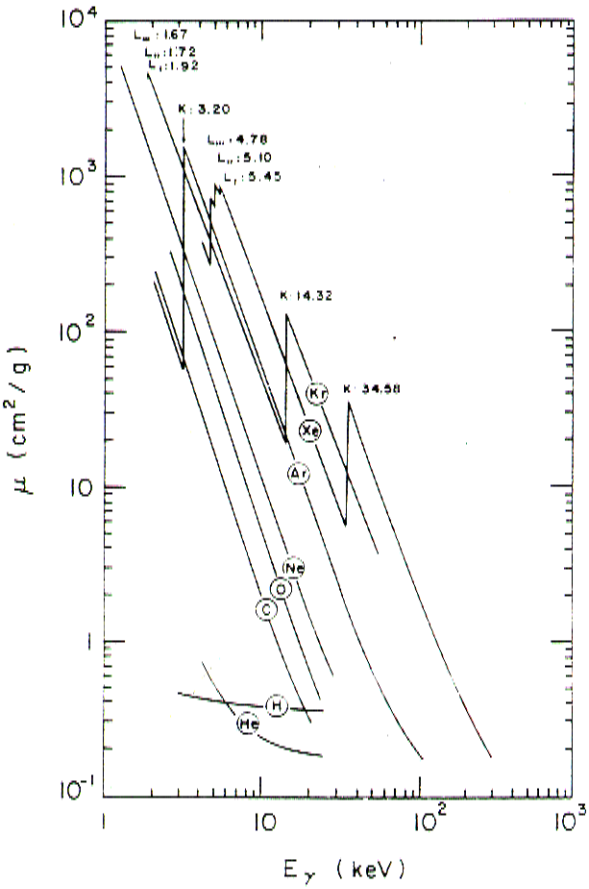

Fig. 11 Absorption coefficient versus energy of photons, in several gases used in proportional counters. Carbon is included, to allow the calculation of absorption in hydrocarbons. The figure has been drawn using the tabulations of Ref. 13.

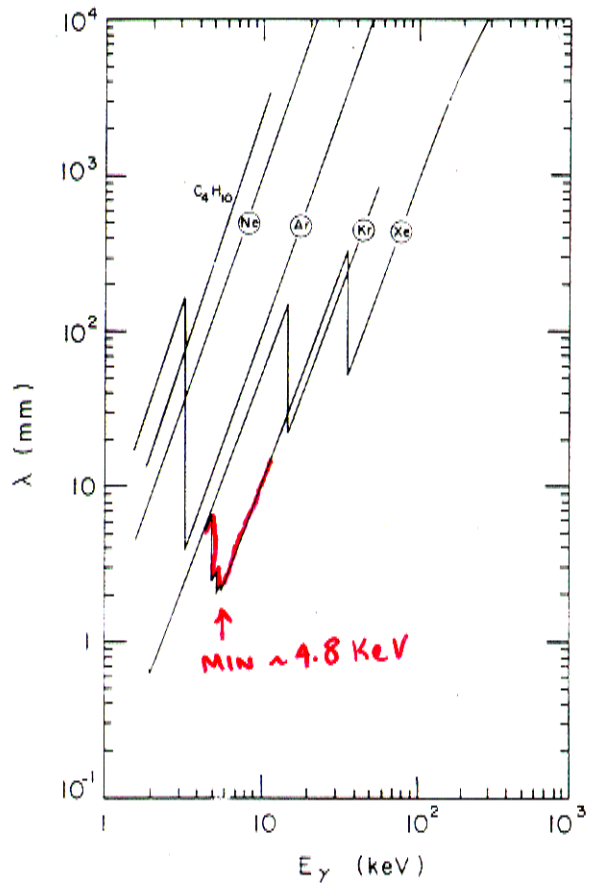

Fig. 12 Mean free path for absorption in several gases at normal conditions, for photons of energy E_γ (from the tabulation in Ref. 13)

SAULI - A CHAPTER IN FERBEL'S BOOK

FOR FINE SAMPLING - NARROW DEPTH -
WE NEED TO CONCENTRATE THE
SPECTRUM IN THIS REGION OR
WE WILL LOSE THE X-RAYS OUT
THE BACK

$$\omega_{max} \simeq \frac{l_1 \omega_1^2}{2\pi c}$$

Table I - Comparison of Various Radiator Materials

Material	Plasma Frequency	l_1 for ω_{max} =4.8 KeV	l_R	single foil(x200)	200 foils	
Lithium	13.85 eV	31 μm	155 cm	1.900	1.563	1.312
CH_2	21.8 eV	12.7 μm	47.9 cm	3.166	1.486	1.116
Mylar	24.8 eV	10.2 μm	28.7 cm	3.517	1.235	.861
Carbon	26.0 eV	8.9 μm	18.8 cm	3.694	1.265	.886

REQUIRE CAPTURE IN 2 PLANE XENON FILLED CHAMBER (90%)

TOTAL INTENSITY RADIATED

$$W = \frac{\alpha}{3} \frac{\hbar (\omega_1 - \omega_2)^2 \gamma}{\omega_1 + \omega_2}$$

since $\omega_1 >> \omega_2$, $W \propto \hbar\omega_1$

NOW $\hbar^2 \omega_1^2 \simeq 2 (Z/A)(\rho/g\,cm^{-3})(21\,eV)^2$

THUS PLASMA FREQ $\sim \sqrt{Z}$

WHILE X-RAY ABS $\sigma \rightarrow Z^{3.5}$

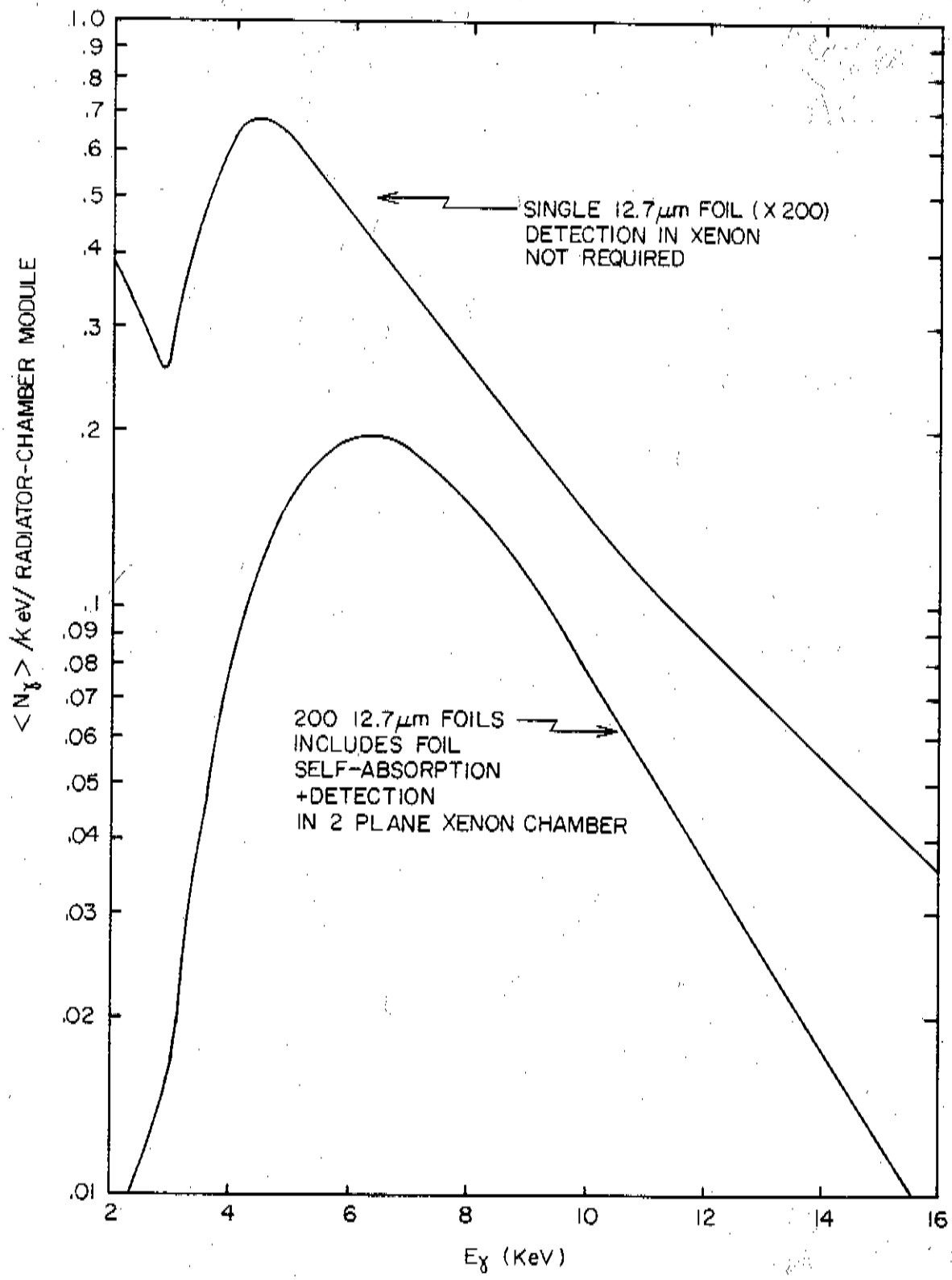
1.0
.9
.8
.7
.6
.5
.4
.3
.2
.1
.09
.08
.07
.06
.05
.04
.03
.02
.01
2
4
6
8
10
12
14
16
E_γ (KeV)
$\langle N_\gamma \rangle$ /K eV/ RADIATOR-CHAMBER MODULE
SINGLE 12.7μm FOIL (X 200)
DETECTION IN XENON
NOT REQUIRED
200 12.7μm FOILS
INCLUDES FOIL
SELF-ABSORPTION
+DETECTION
IN 2 PLANE XENON CHAMBER

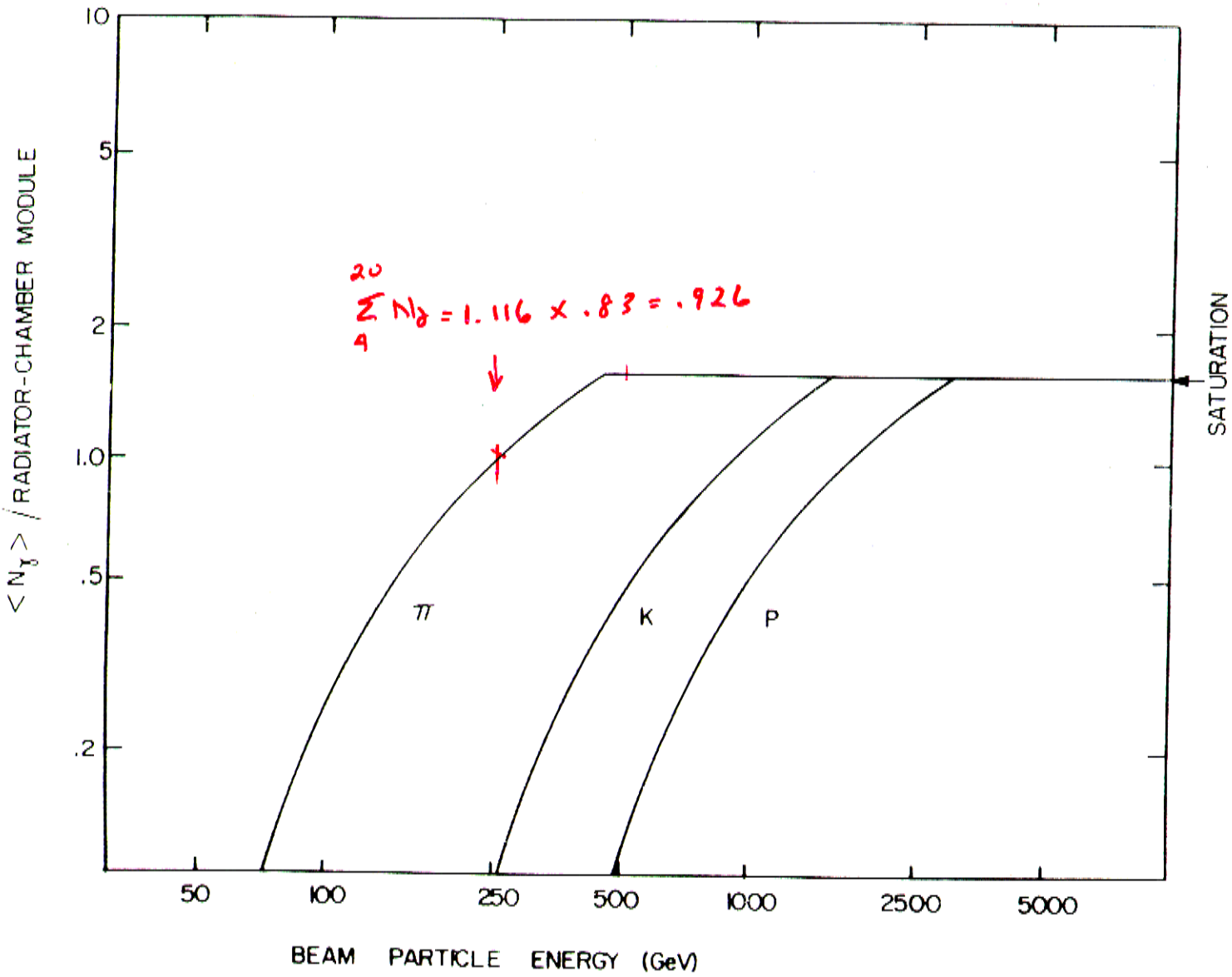

$\gamma_{SAT} \sim \sqrt{l_1 l_2}\, \omega_{p_1} \doteq 3126$ for us

$\simeq 8770$ for E715 → 4.5 GeV e's

(thicker foils/wider gaps)

Improvement in kaon-pion separation using a new technique with transition radiation detectors, from an experiment by a CERN/Moscow group. Rather than measuring total ionization charge (right), the new method (left) concentrates instead on the detection of clusters of intense ionization.

CERN COURIER

SEPTEMBER 1980

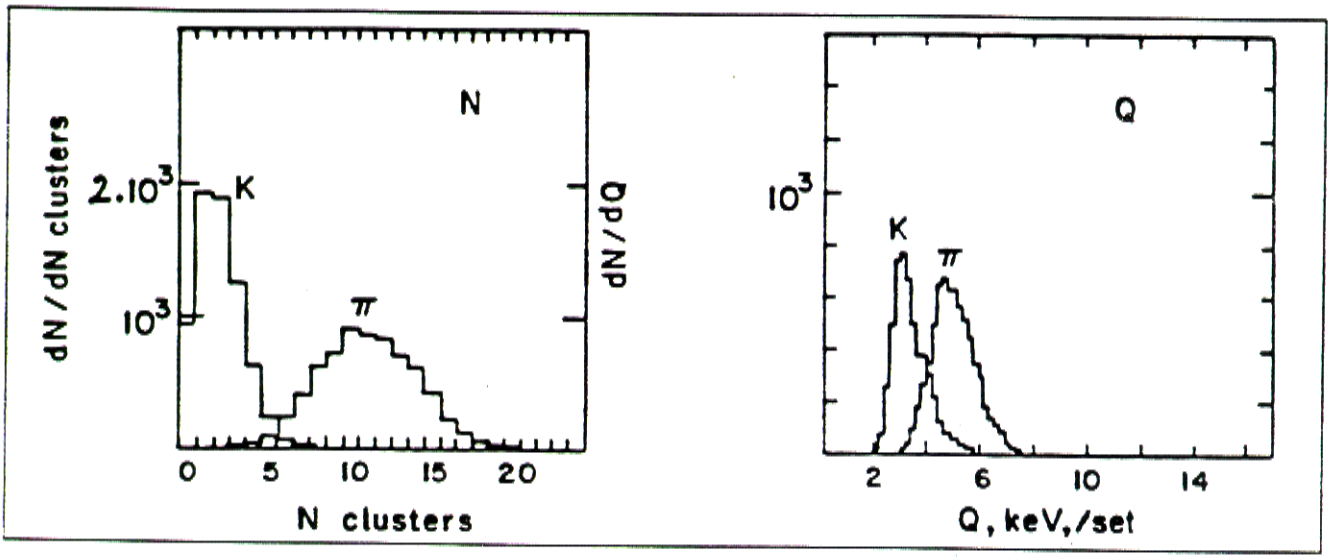

"CLUSTER COUNTING" –

REFS – C. FABJAN et.al., "PRACTICAL PROTOTYPE OF A CLUSTER-COUNTING TRANSITION RADIATION DETECTOR", NIM 185 (1981) 119.

T. LUDLAM et.al., "PARTICLE IDENTIFICATION BY ELECTRON CLUSTER DETECTION OF TRANSITION RADIATION PHOTONS", NIM 180 (1981) 413.

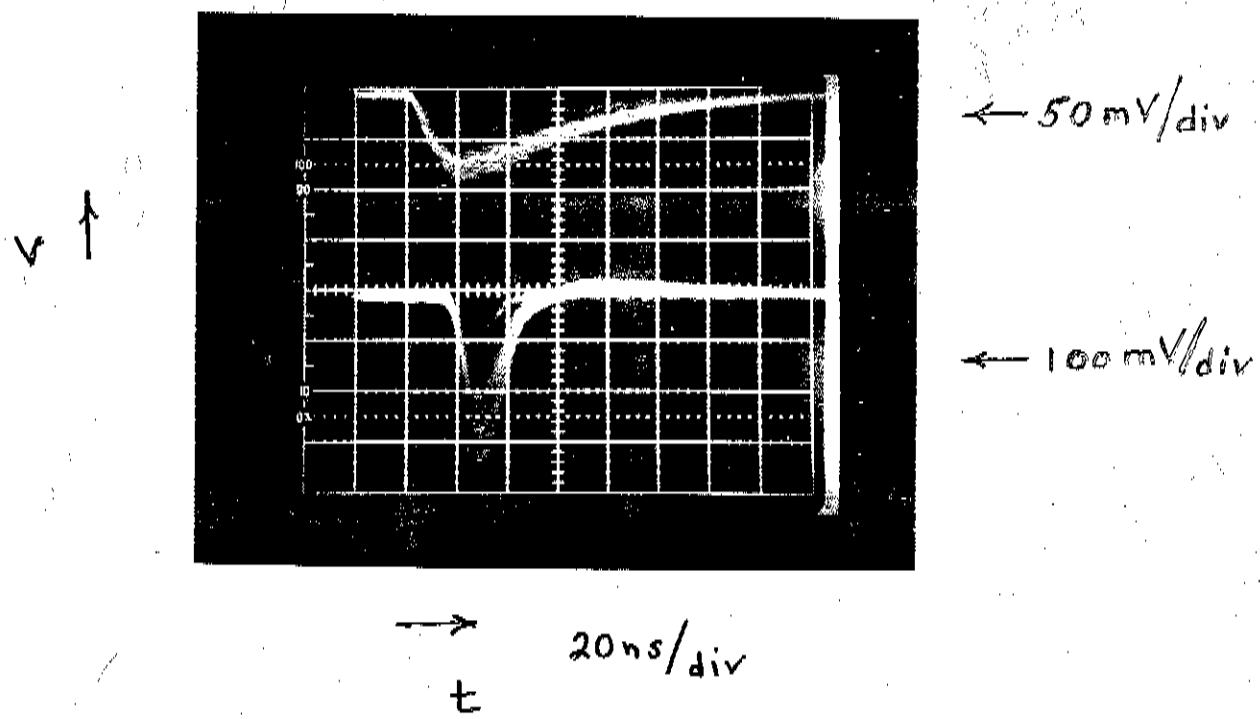

^{55}Fe fwhm ~ 26ns ON THE BOTTOM TRACE WHICH IS THE A-S-D ANALOG OUT

UPPER TRACE SHOWS THE PREAMP OUTPUT

GAS - Xe 99.9% PURE BUBBLED THROUGH METHYLAL AT 0°C - ~ 90% Xe

VOLTAGE - 2650 V - GAS GAIN ~ 2×10^4

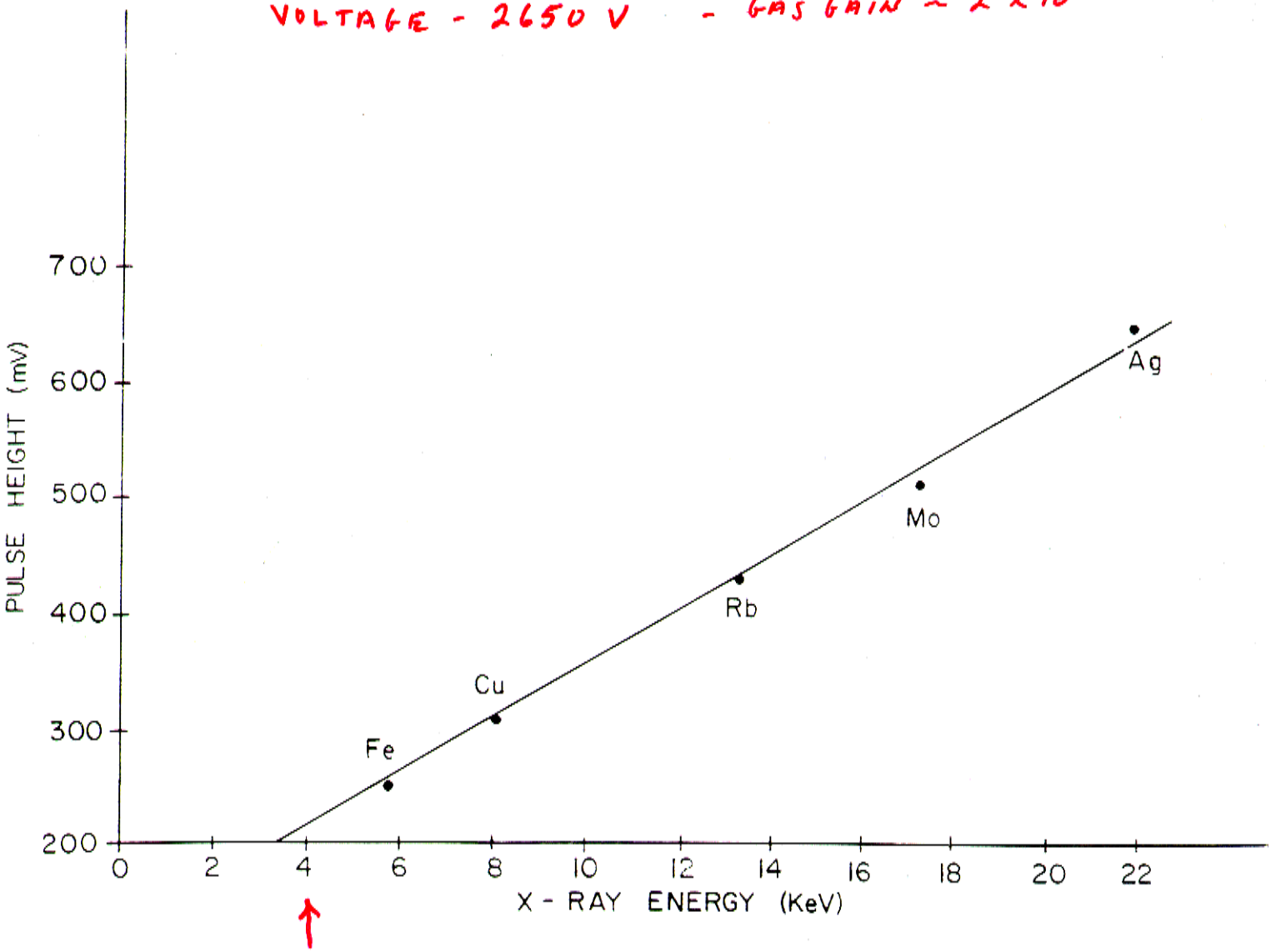

THRESHOLD

4 KeV ≈ 215 mV

(SINCE SIGNAL WAS DIVIDED IN TWO FOR A SELF-TRIGGER, THE ACTUAL THRESHOLD ON THE DISCRIMINATOR WAS ~430 mV)

MEASURED EFFICIENCY FOR X-RAY CAPTURE SIGNAL TO BE ABOVE THRESHOLD WAS 83% INDEPENDENT OF ENERGY

WE ALSO EXPOSED THE CHAMBER TO A β SOURCE Ru^{106} WHERE THE β IS MINIMUM IONIZING

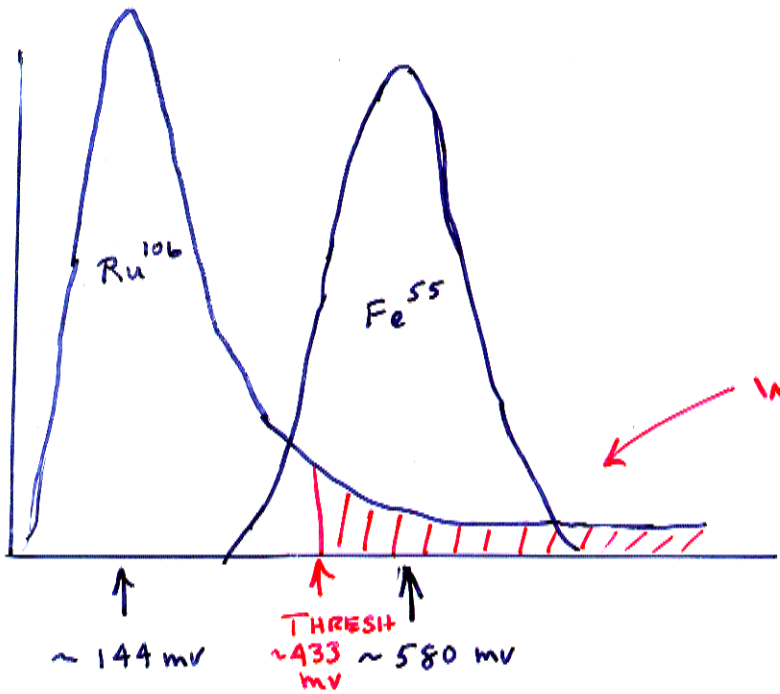

WITH THIS THRESHOLD, THE SIGNAL DUE TO IONIZATION ALONG THE PARTICLE PATH YIELDS A SIGNAL 8.2% OF THE TIME

ACCORDING TO SAULI'S CHAMBER ARTICLE

IONIZATION IN Xe IS 6.76 keV/cm (44 np/cm)

WE ARE INTEGRATING OVER ~ 2mm OF PATH $= 1.35\ \text{keV} \times \frac{433\ \text{mv}}{4\ \text{keV}} = 146\ \text{mv}$

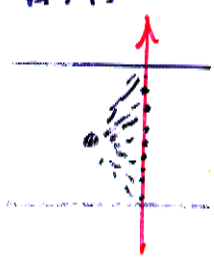

SYSTEM - 24 MODULES LIKE THIS

TOTAL LENGTH 2.79 m

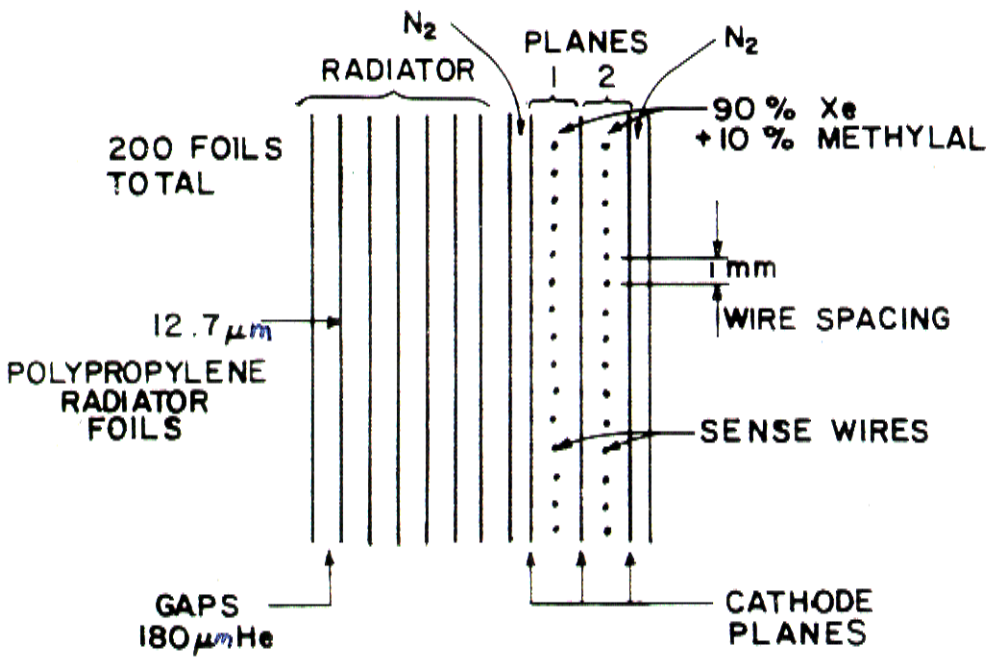

8.3 % λ

16.9 % X_0

INCLUDES 2 1/8" SCINTILLATOR PADDLES

USED IN FRONT & BACK OF

THE TRD FOR GATING

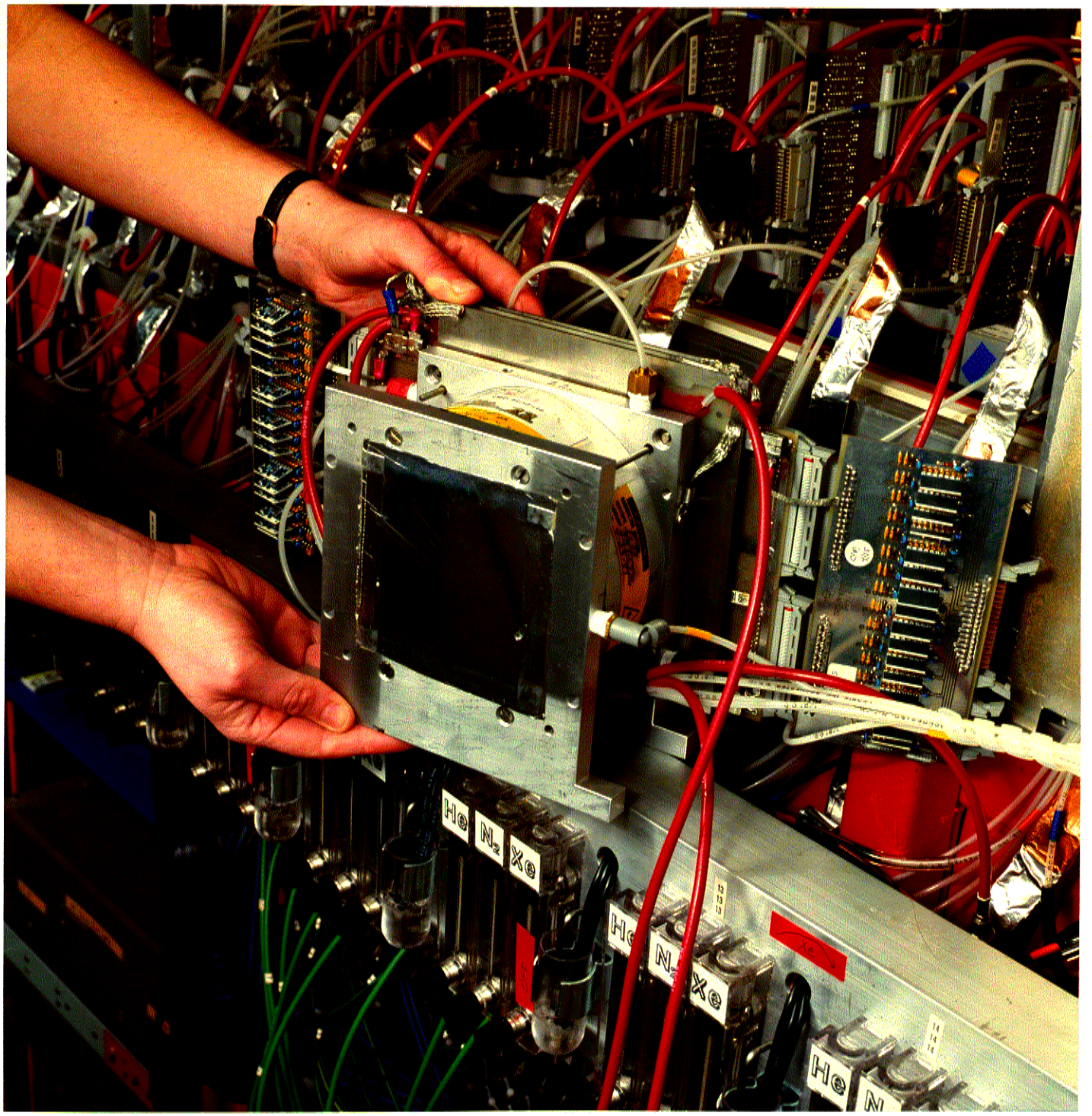

88-489-4

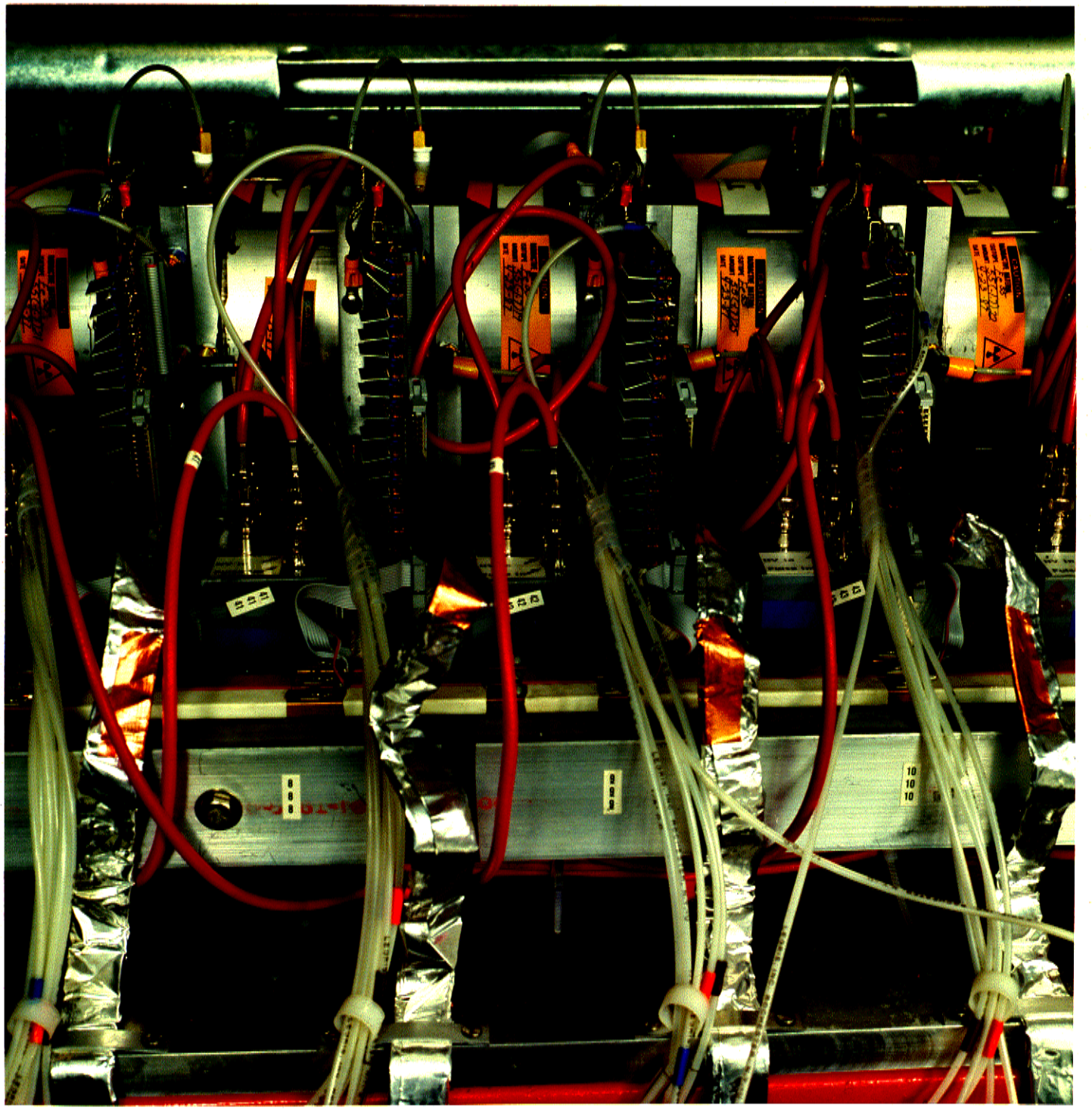

88-489-9

88-489-9

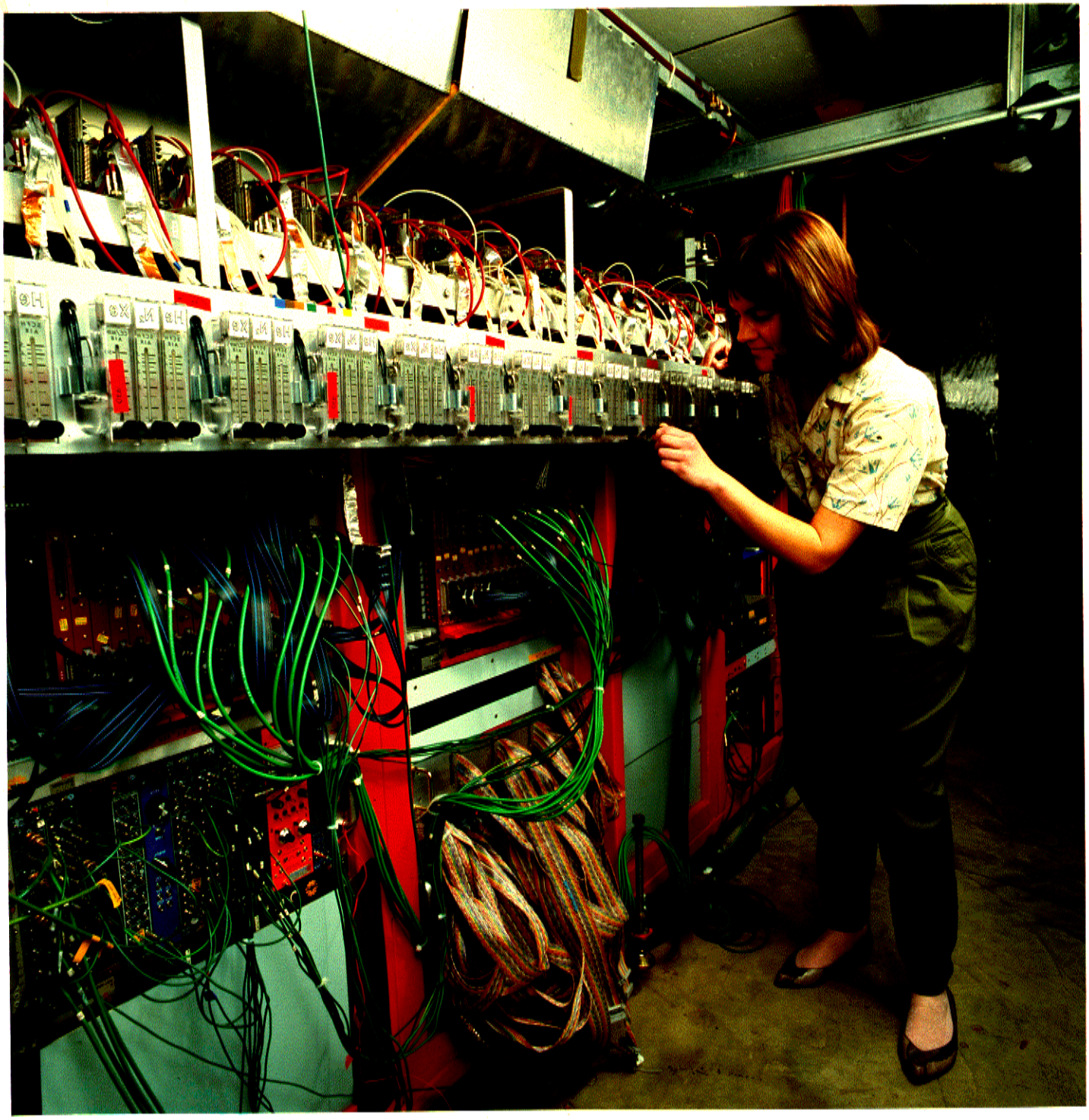

88-488-1

Plane by Plane Comparison of Data and Monte Carlo

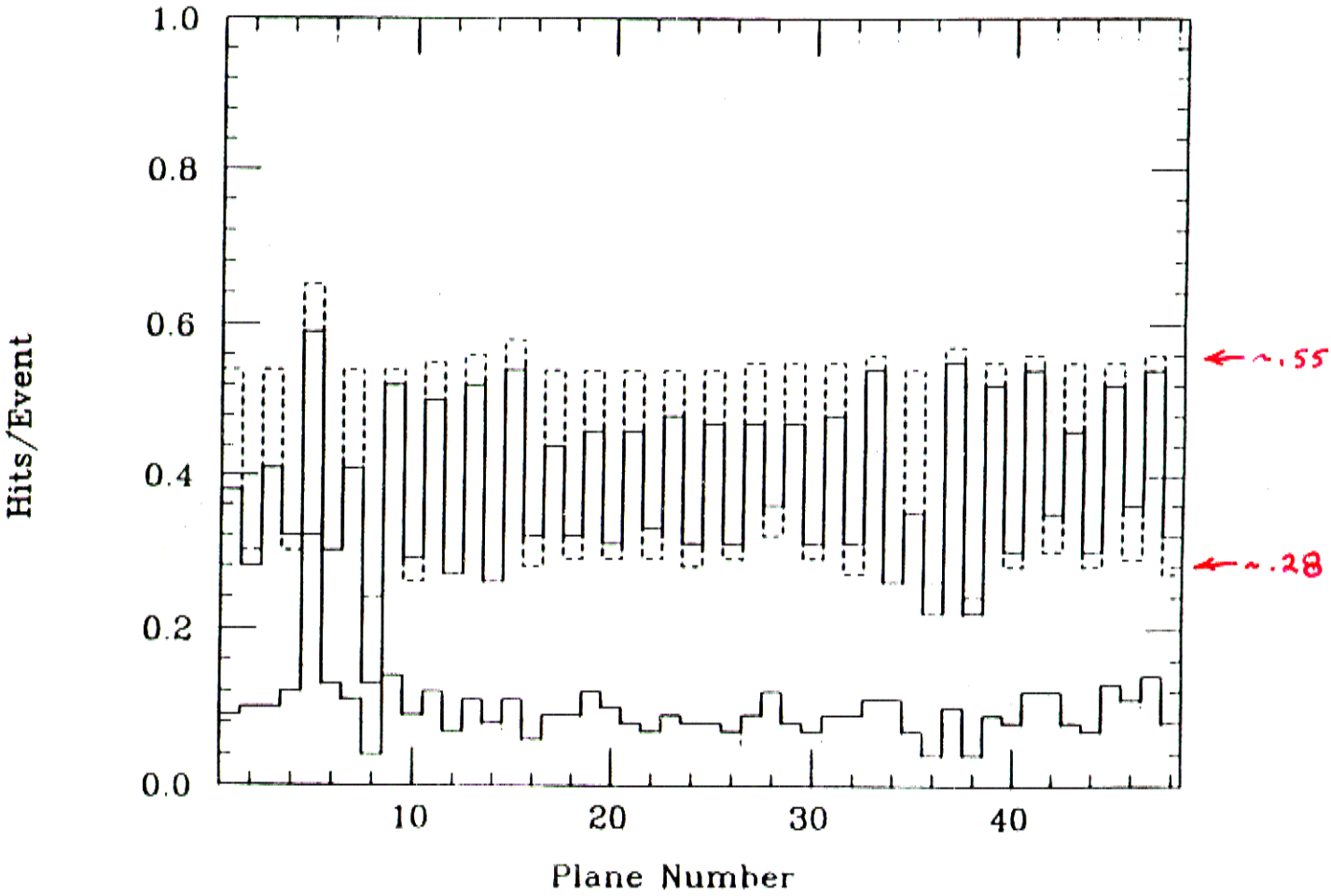

MORE TR SEEN IN FRONT PLANES
SINCE FEWER REMAIN TO BE
DETECTED IN SECOND

TEND TO OVERPREDICT FRONT PLANE
RESPONSE + UNDER PREDICT REAR

Σ OF TWO AGREES PRETTY WELL

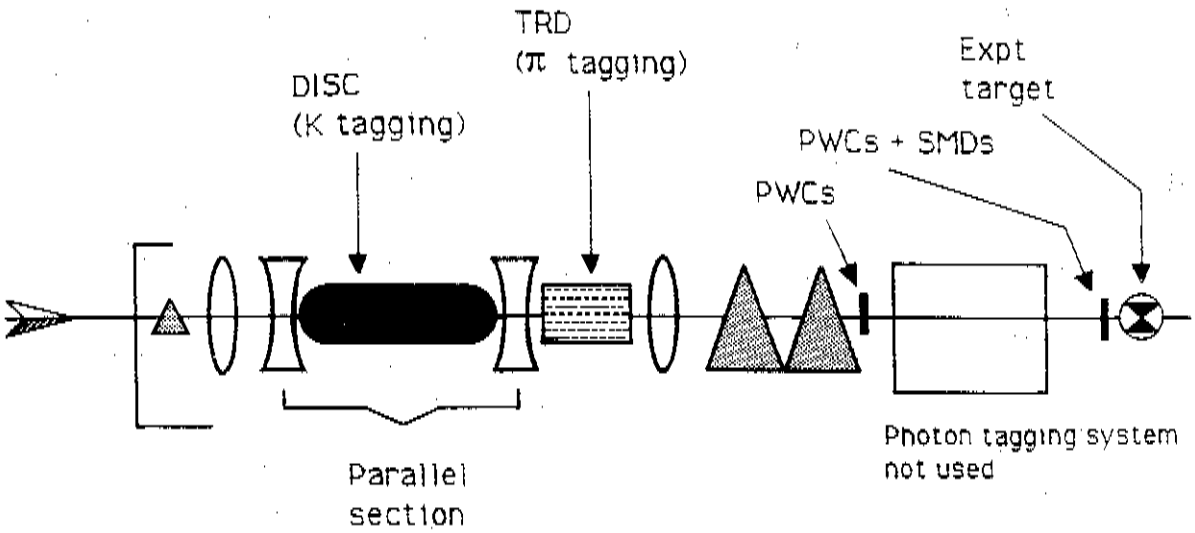

Enclosure PE5

FOR THE POSITIVE BEAM π's, K's, p's

TWO TAGGING DETECTORS WERE

REQUIRED

A DIFFERENTIAL ISOCHRONOUS SELF-FOCUSING

CERENKOV COUNTER (DISC)

AND THE TRD

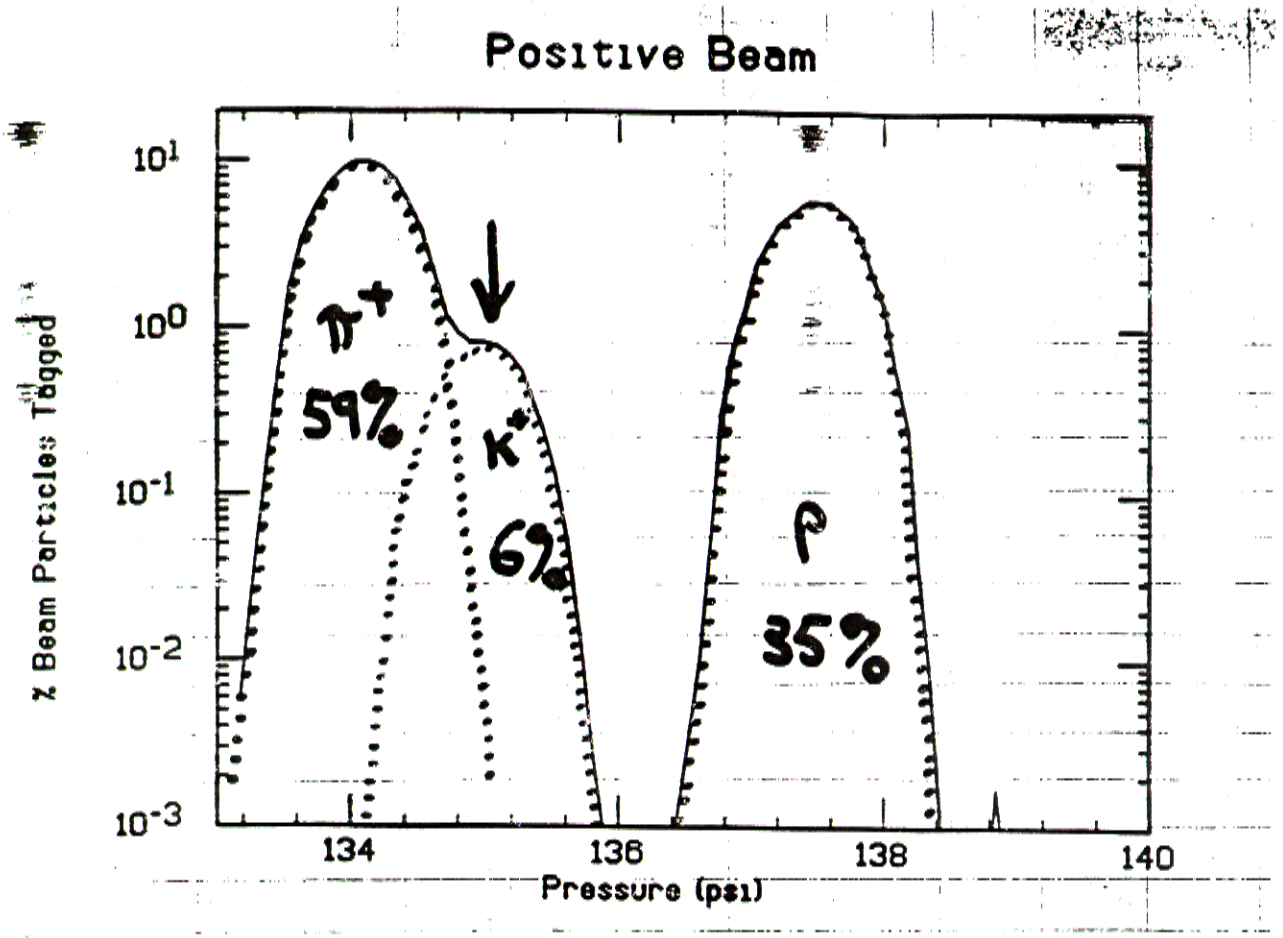

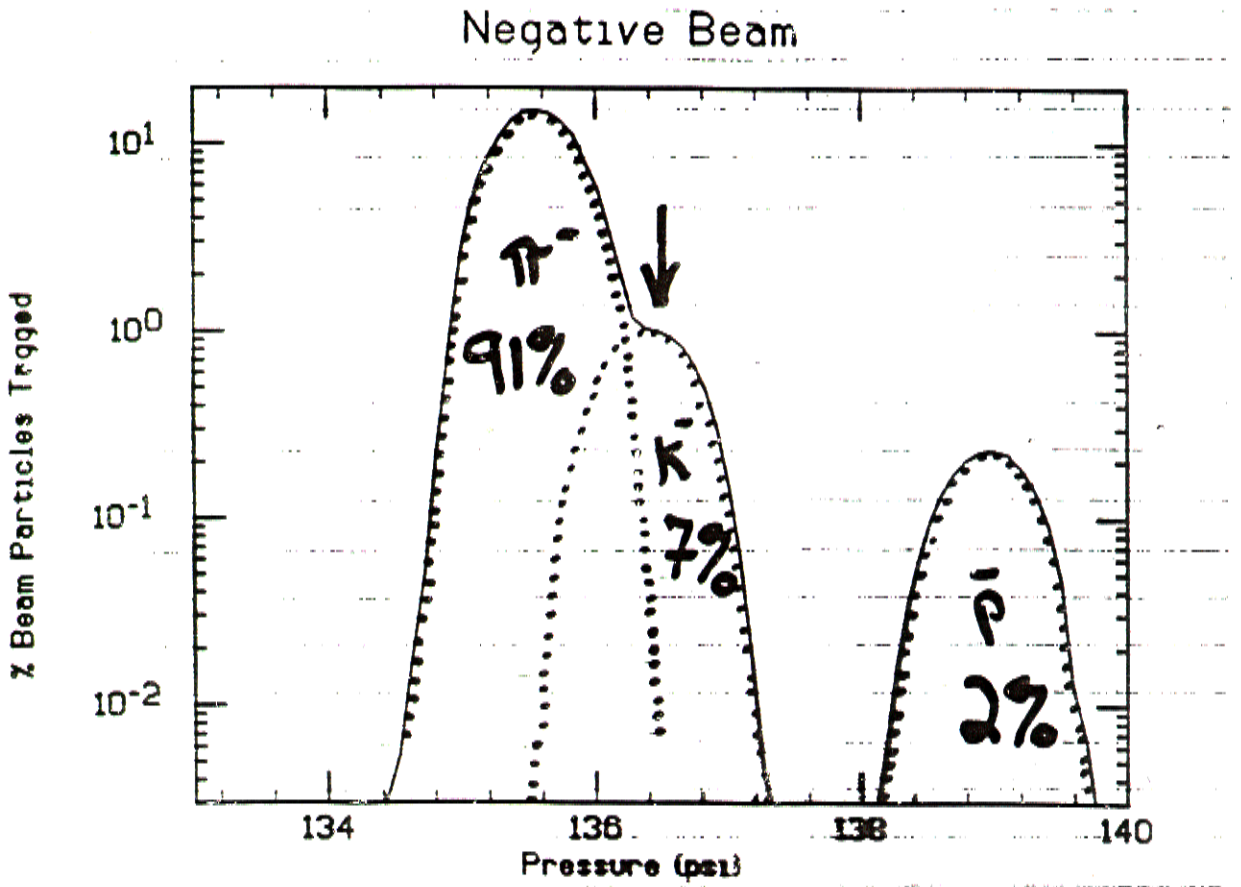

ARROWS SHOW SET POINTS FOR ORDINARY DATA TAPES
SPECIAL TAPES FOR TRD CALIBRATION WERE TAKEN FOR
P'S AND π'S.

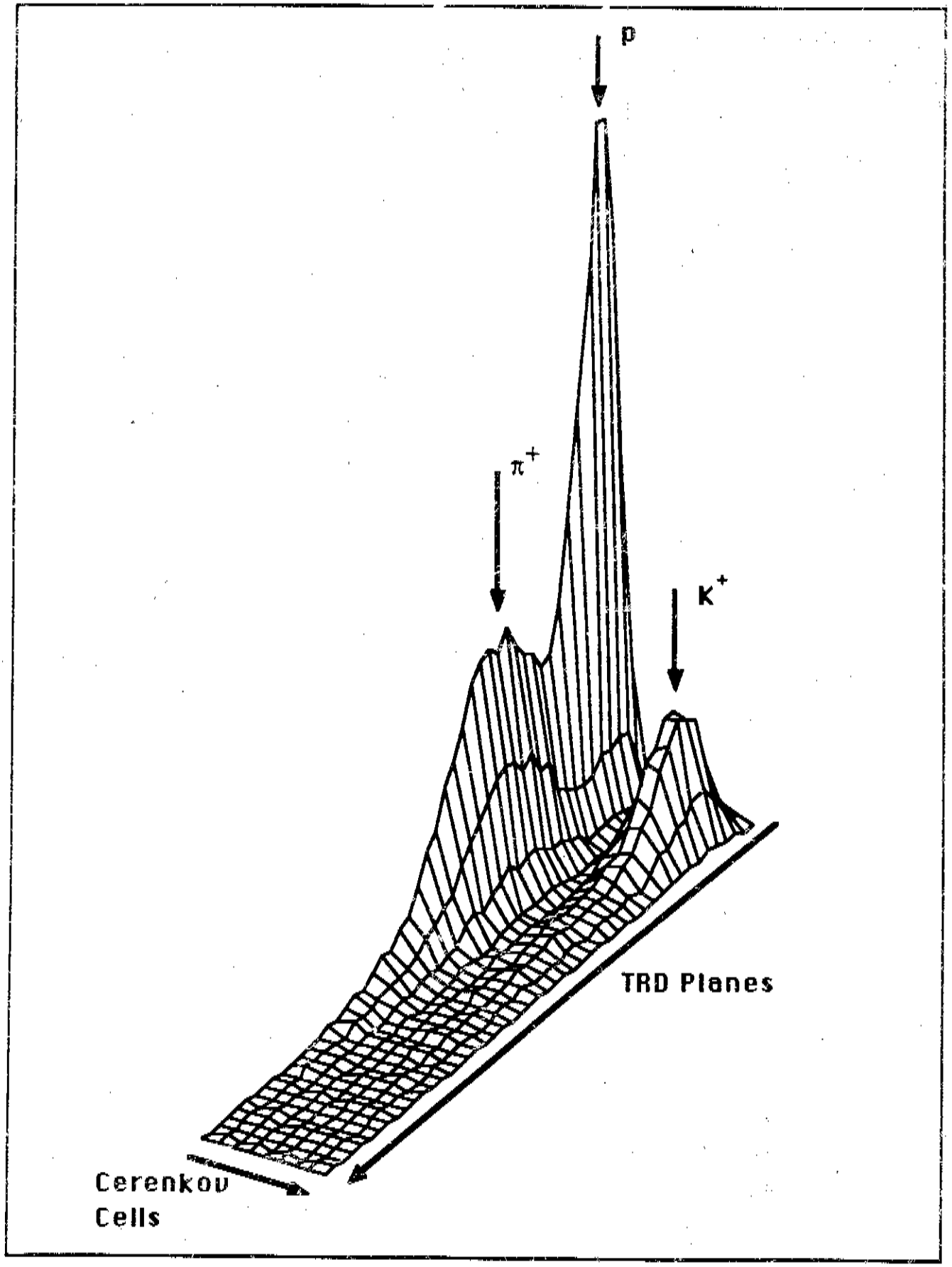
p
π^+
K^+
TRD Planes
Cerenkov
Cells

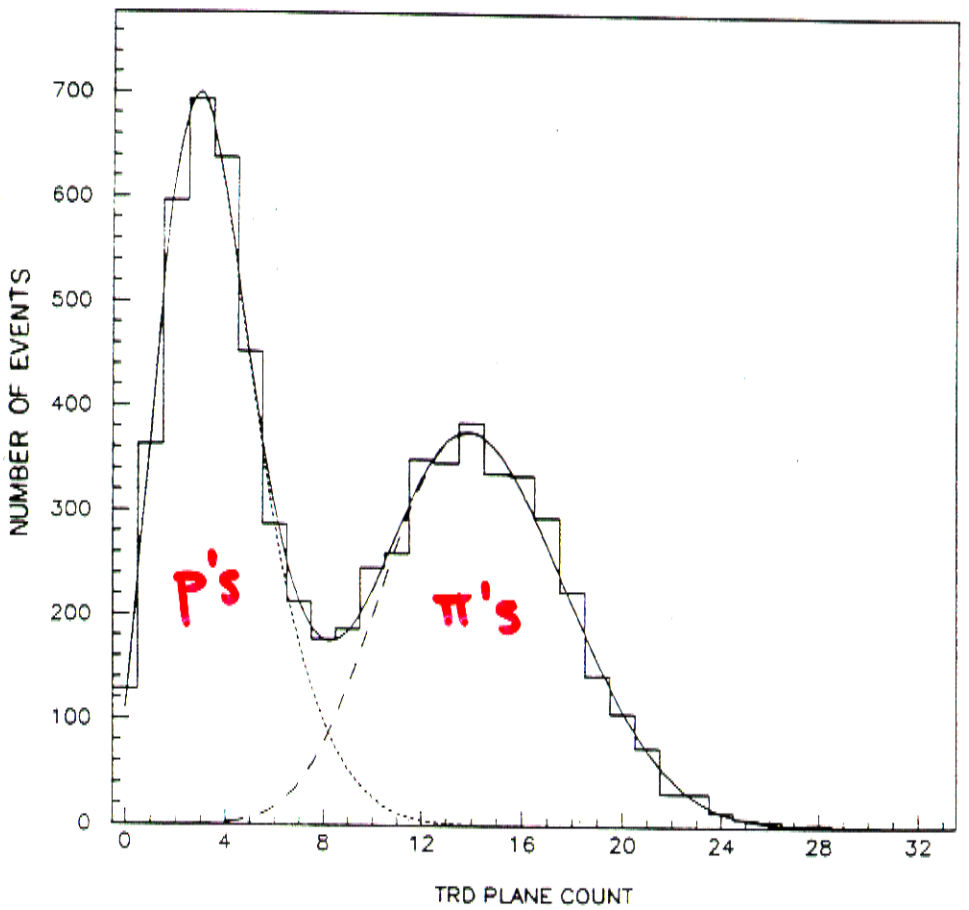

NO DISC TAG - SAME DATA TAPE

Table II - TRD Performance

Pions

# of TRD Planes That Fired	Pion Efficiency		Proton Contamination	
	Expt.	Fit	Expt.	Fit
≥ 8	.946	.948	4.13%	4.07%
≥ 10	.868	.868	2.23%	2.19%
≥ 12	.733	.730	1.75%	1.75%

Protons

# of TRD Planes That Fired	Proton Efficiency		Pion Contamination	
	Expt.	Fit	Expt.	Fit
< 6	.875	.875	2.00%	1.82%
< 7	.934	.929	3.26%	3.14%
< 8	.962	.957	5.48%	5.28%

↑

PION / PROTON FRACTIONS USED ARE FOR ET TRIGGERS .493/.507

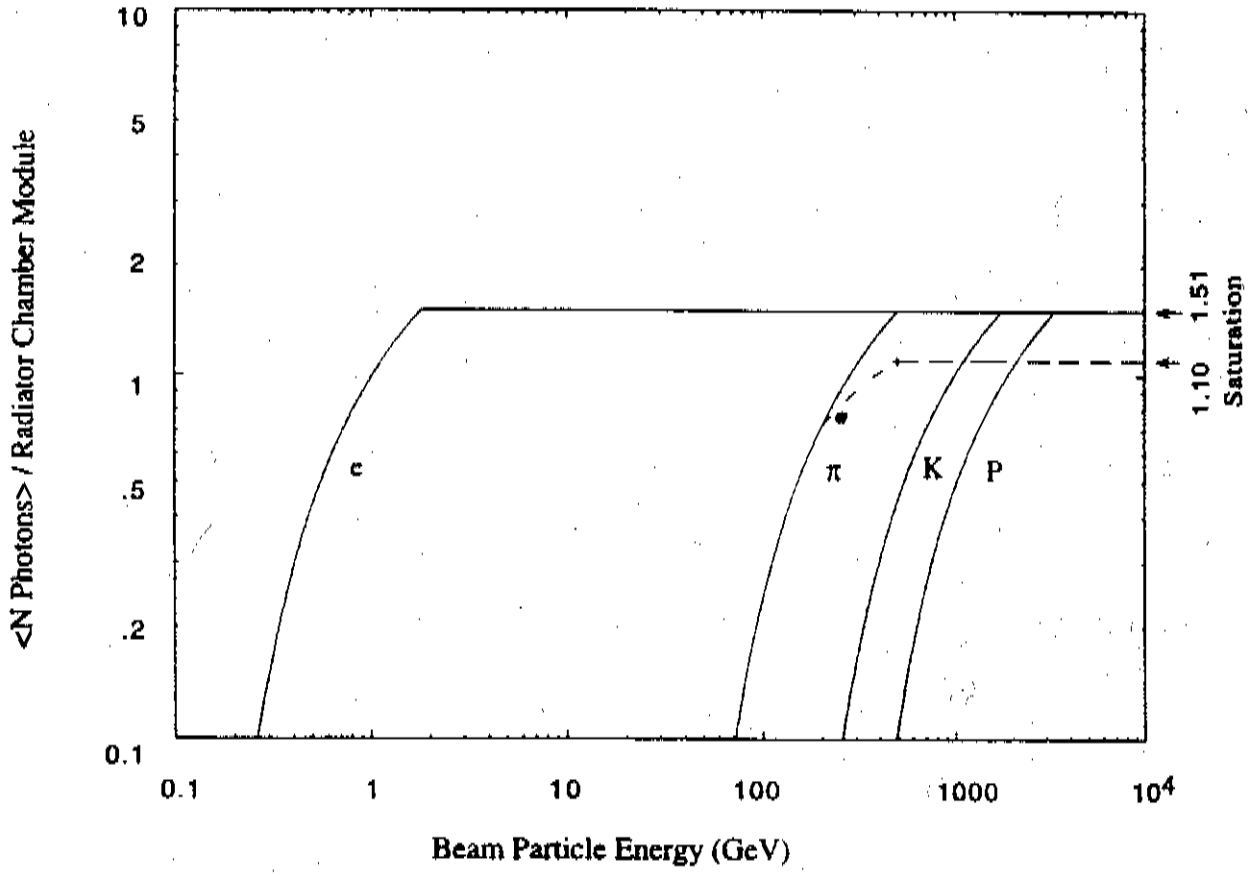
<N Photons> / Radiator Chamber Module
10
5
2
1
.5
.2
0.1
0.1
1
10
100
1000
10^4
Beam Particle Energy (GeV)
e
π
K
P
1.51
1.10
Saturation

E715 - IDENTIFY e's $\epsilon_e \sim 99\%$

VOROBYOV

REJECT π's $\epsilon_\pi / \epsilon_e \sim 10^{-3}$

TO SELECT $\Sigma^- \to n e^- \bar{\nu}$ VS $\Sigma^- \to n \pi^-$,

WHICH IS $\sim 10^3$ MORE PROBABLE

IN THE 5 - 80 GeV range $\gamma \gtrsim 10^4$

E761 - DETERMINATION OF SHOWER POSITION

E781 - IDENTIFICATION OF SECONDARY e's

AS ABOVE FOR LEPTONIC DECAYS OF

CHARM BARYONS

- IDENTIFICATION OF BEAM π's

TO ALLOW SELECTION OF Σ^- INCIDENT

Σ^- / π^- RATIO 70% / 30%

600 GeV BEAM $\sim 10^6$ Σ^-/SEC

E715

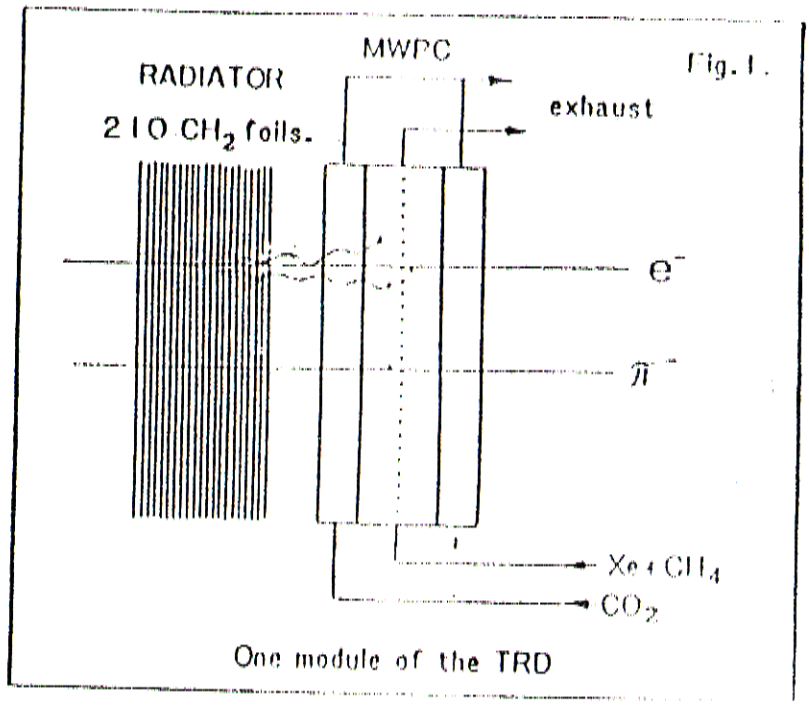

210 CH_2 foils, 17 μm thick, separated by 1.0 mm He gaps

12 Modules

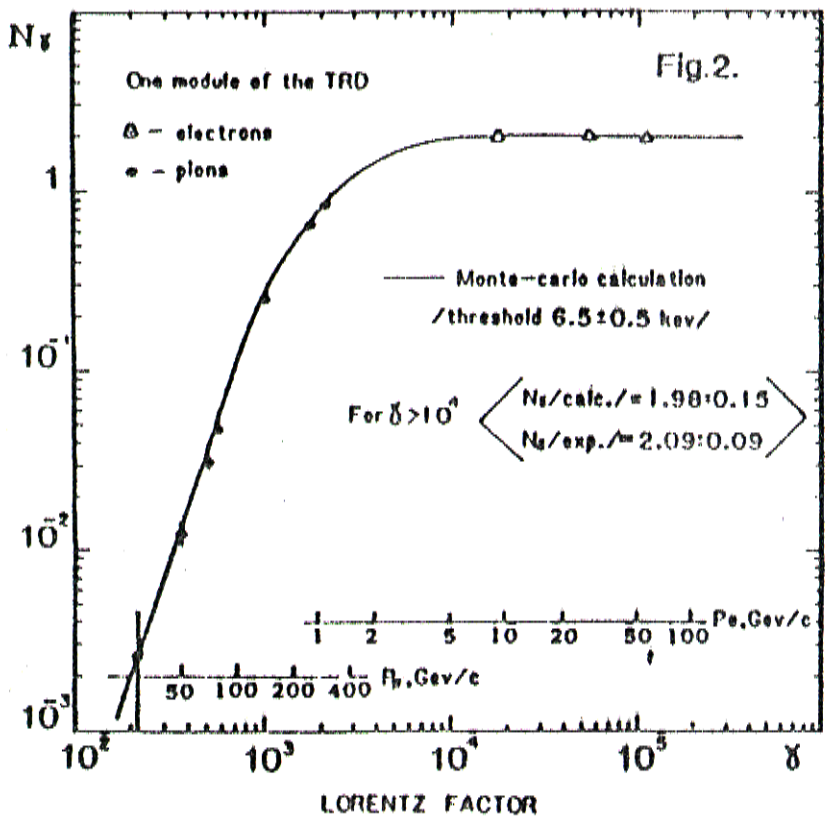

$\gamma_{SAT} \simeq 8770 \sim 10^4$

N_γ / module $\simeq 2$

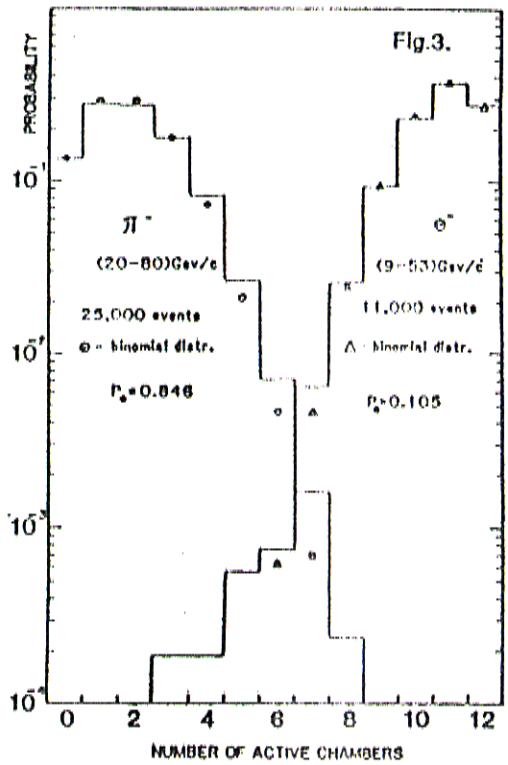

$N_{ac} \geq 7$

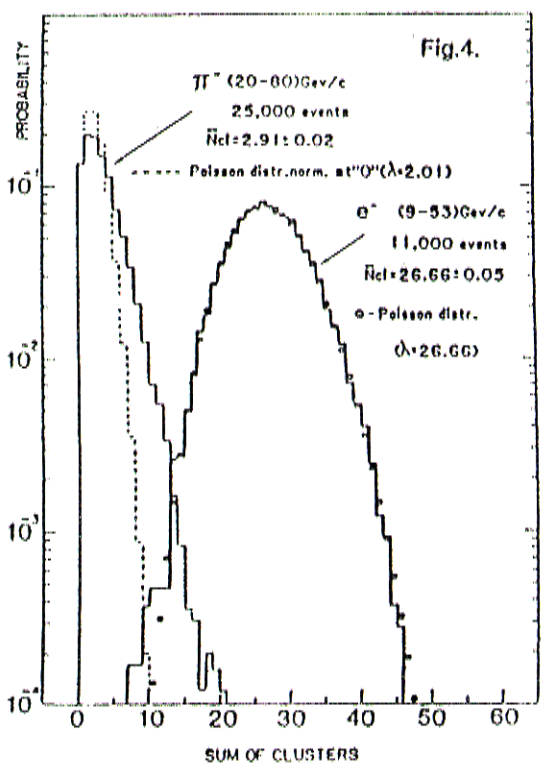

$N_{cl} \geq 12$

ONLINE REQUIREMENTS

$\Rightarrow$ REJECTION FACTOR OF 40

E715

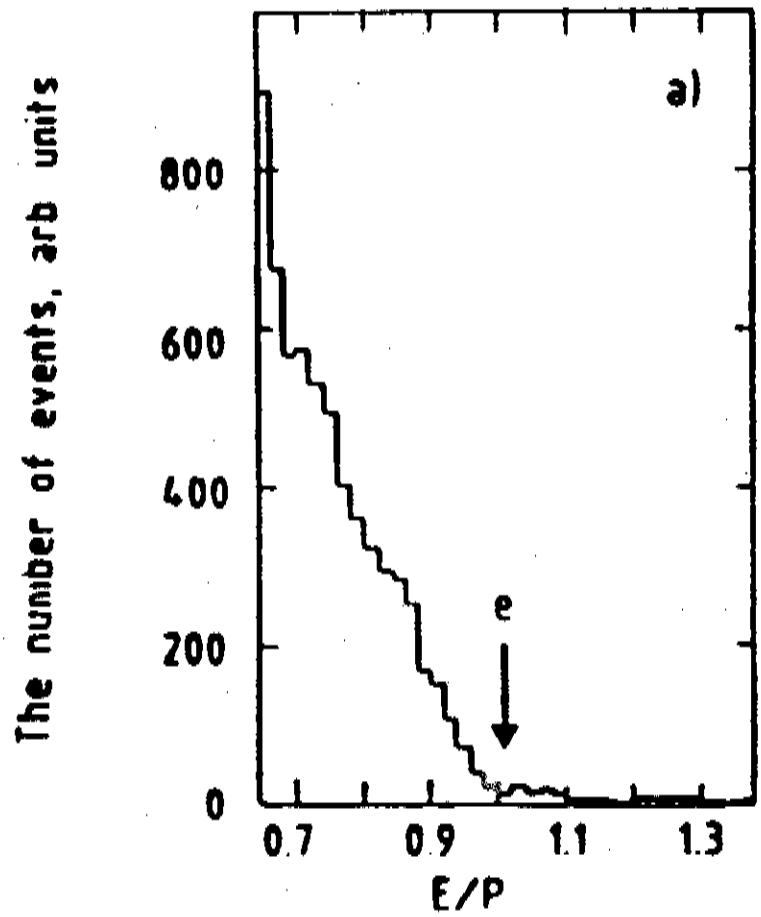
a)
The number of events, arb units
800
600
400
200
0
e
0.7
0.9
1.1
1.3
E/P

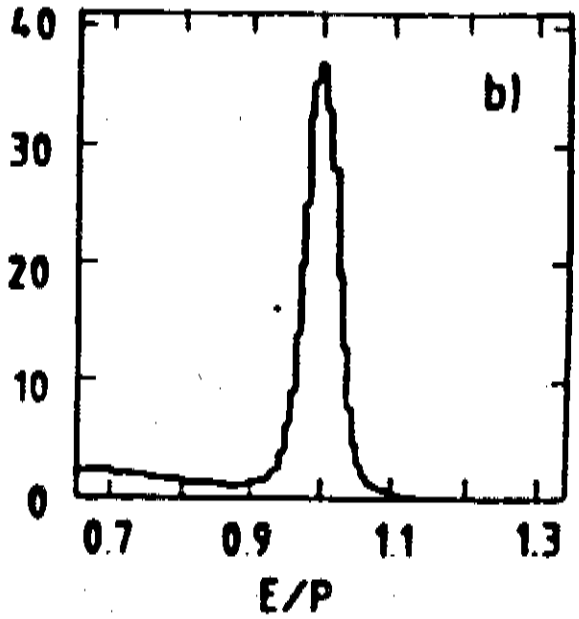
b)
40
30
20
10
0
0.7
0.9
1.1
1.3
E/P

KTeV

Figure 1: Cross sectional plan of KTeV TRDs.

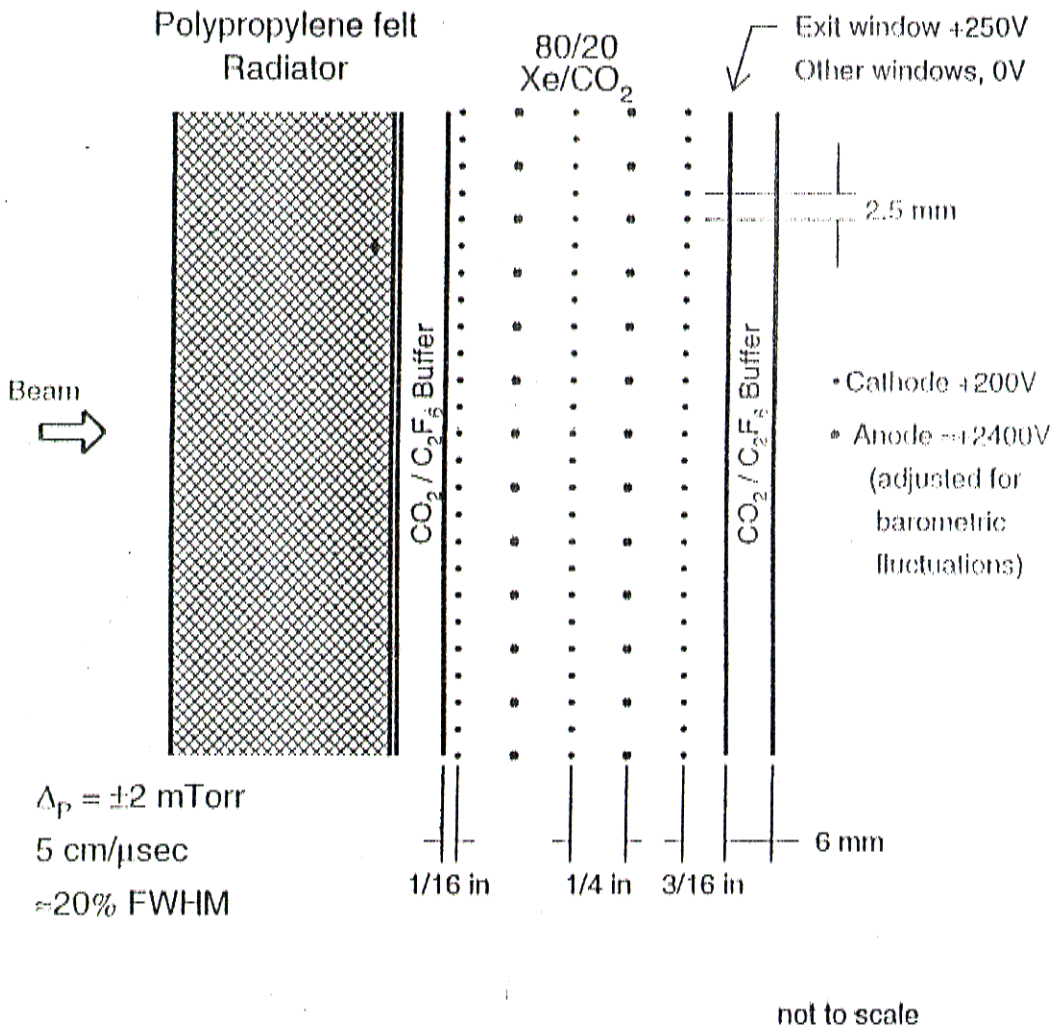

8 or 9 modules like this

Reject π's in backgrounds to

$K_L \rightarrow \pi^0 e^+ e^-$ decays.

π and e from identified Ke3 decays

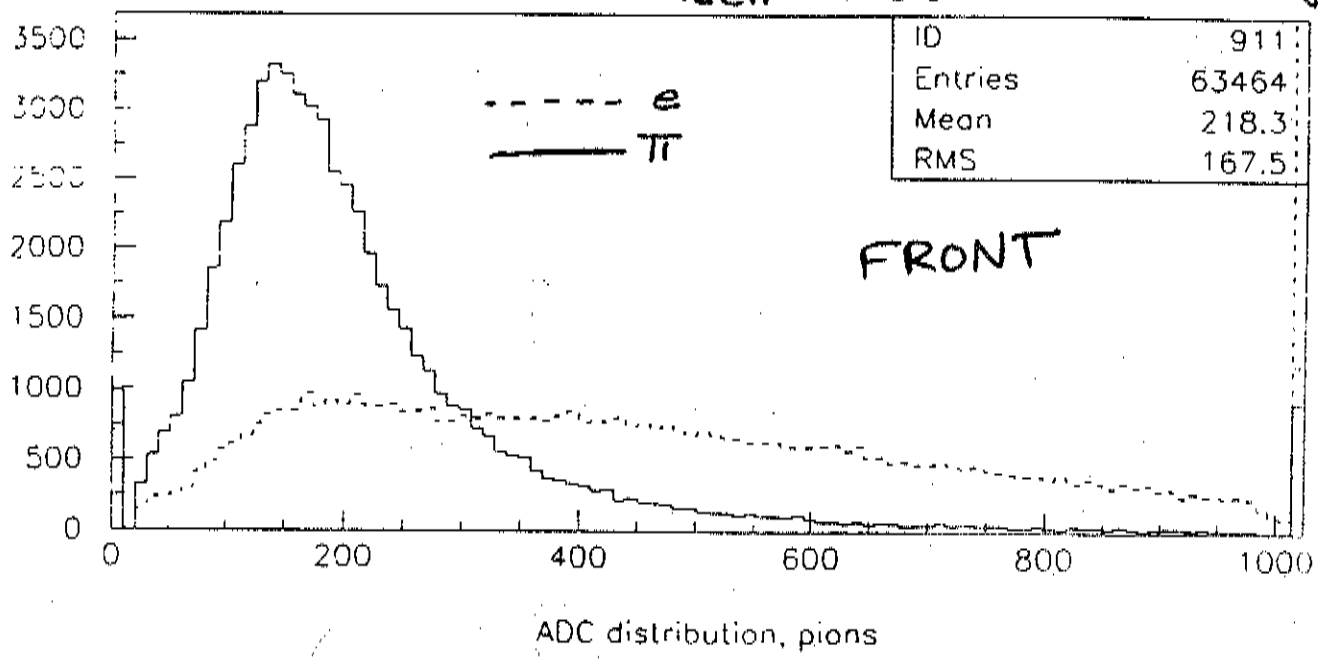

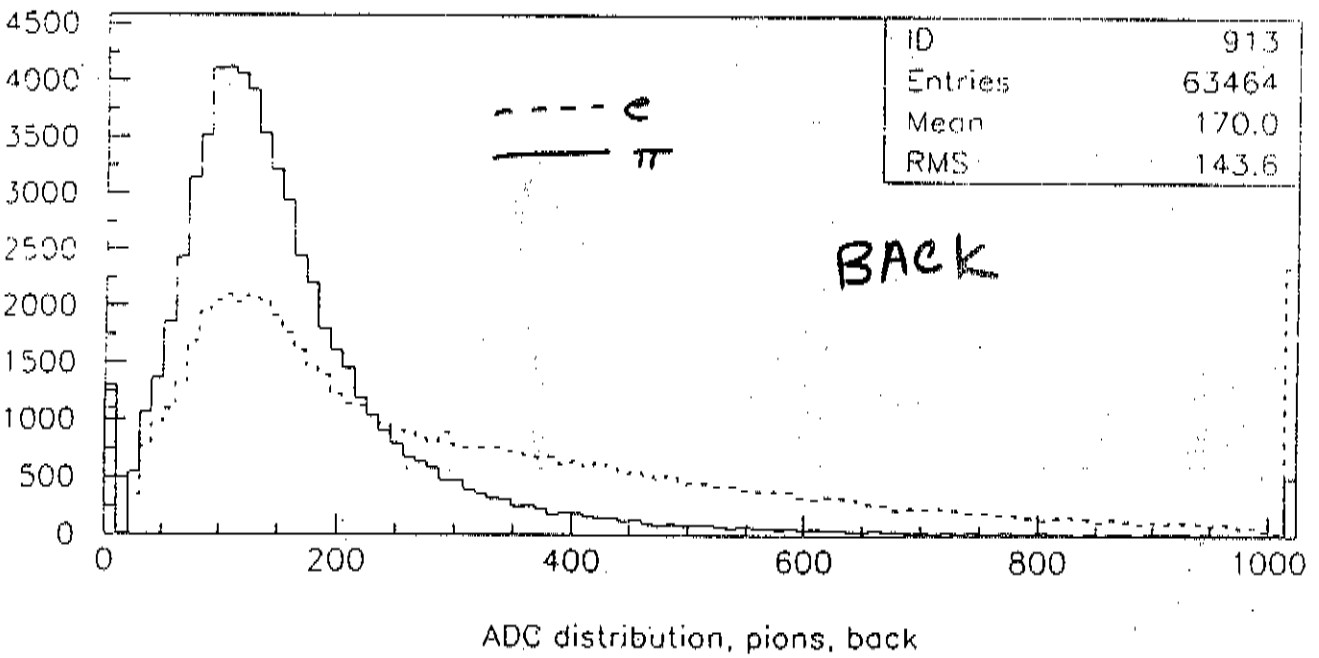

Ke3 events from KTeV Run 5636 – Preliminary

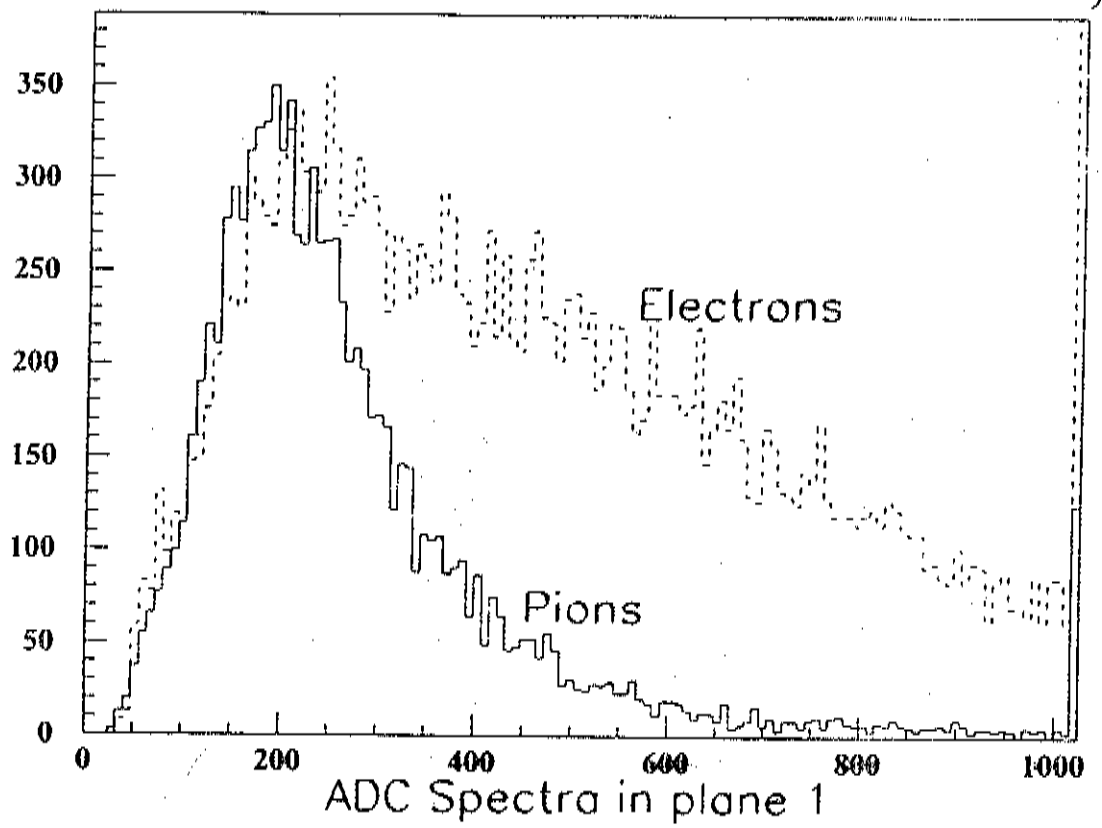

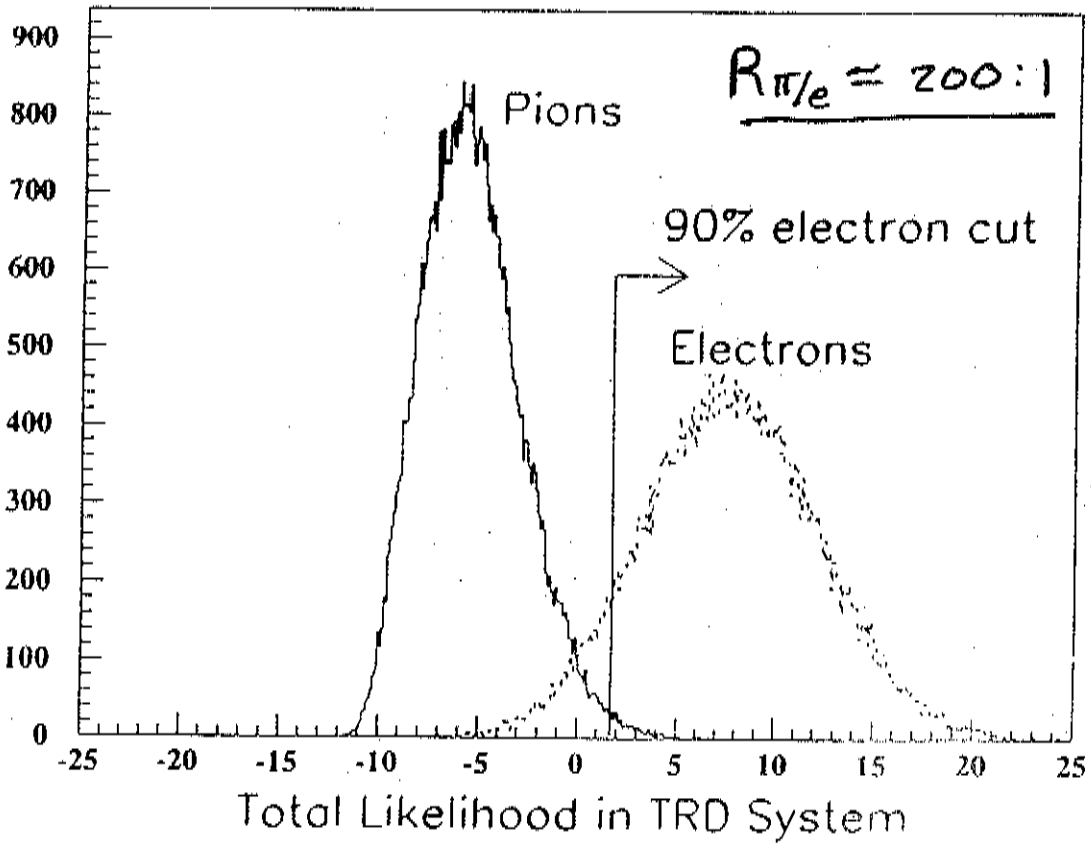

KTeV Run 5636 : Minimum Bias Trigger

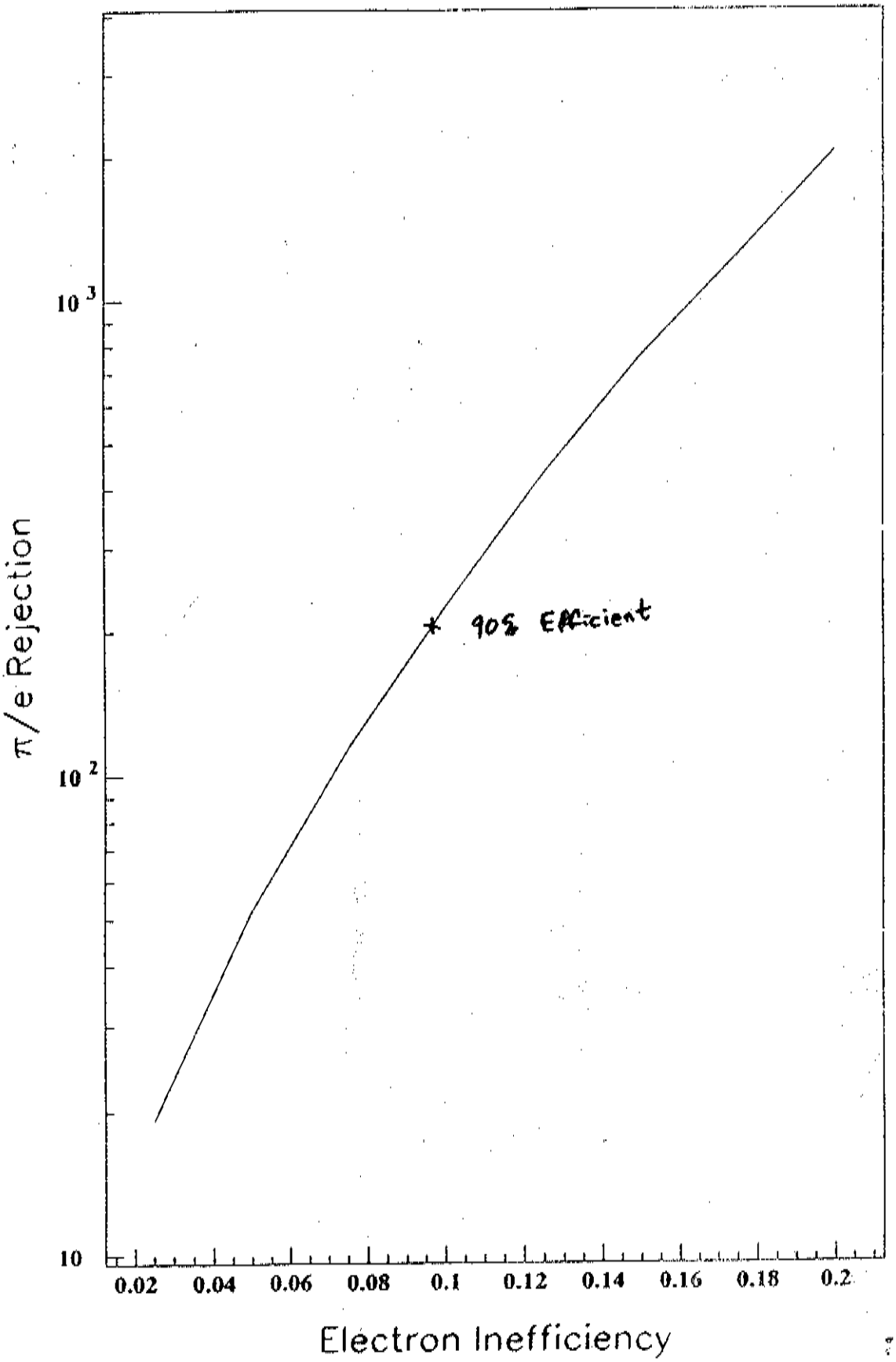

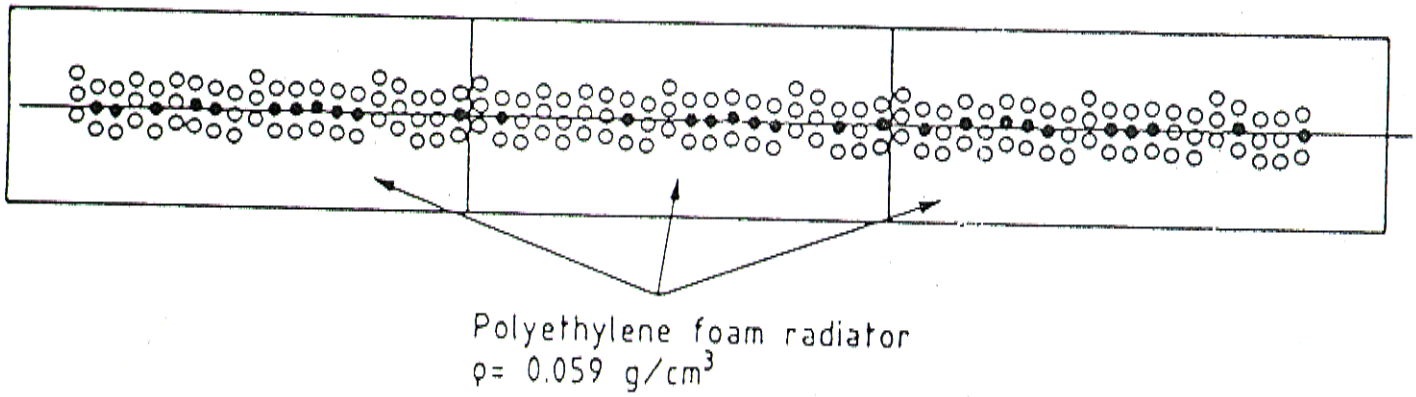

Fig. 3. Event display of a single particle crossing the TRD prototype.

COMBINED FUNCTION DETECTOR

2 OR 3 THRESHOLDS

TRACKING AND PARTICLE ID

CAN SEE ELECTRONS IN JETS

J. T. SHANK et al, NIM A309 (1991) 377

WHY TRD'S?

TRD's are versatile

- wide window for electron ID
- narrow (but useful) window for hadron ID

TRD's are relatively fast

- (and may be made faster)
- can be used in the trigger

TRD's have multiple functionality

- e.g., TRD/Tracker
- Preshower Detector